Supporting information

for

Glutathione-Responsive Prodrug Nanoparticles for Effective Drug Delivery and Cancer Therapy

Xiang Ling,[†] Jiasheng Tu,[‡] Junqing Wang,[†] Aram Shajii,[†] Na Kong,[†,§,#] Chan Feng,[†] Ye Zhang,[†] Mikyung Yu,[†] Tian Xie,[§,*] Zameer Bharwani,[†] Bader M. Aljaeid,[⊥,*] Bingyang Shi,[†] Wei Tao,[†,*] and Omid C. Farokhzad[†,*]

[†]Center for Nanomedicine and Department of Anesthesiology, Brigham and Women's Hospital, Harvard Medical School, Boston, Massachusetts 02115, United States.
[‡]Center for Research Development and Evaluation of Pharmaceutical Excipients and Generic Drugs, Department of Pharmaceutics, State Key Laboratory of Natural Medicines, China Pharmaceutical University, Nanjing, Jiangsu 210009, China.
[§]Department of Cancer Pharmacology, Holistic Integrative Pharmacy Institutes, College of Medicine, Hangzhou Normal University, Hangzhou, Zhejiang 310012, China.
[#]Sir Run Run Shaw Hospital, Zhejiang University School of Medicine, Hangzhou, Zhejiang 310000, China.
[⊥]Department of Pharmaceutics, Faculty of Pharmacy, King Abdulaziz University, Jeddah, Saudi Arabia.

* Corresponding authors: tianxie@hznu.edu.cn (T.X.); baljeaid@kau.edu.sa (B.M.A.); wtao@bwh.harvard.edu (W.T.); ofarokhzad@bwh.harvard.edu (O.C.F.)

METHODS

Materials

Cisplatin, acetic anhydride, butanoic anhydride, hexanoic anhydride, octanoic anhydride, decanoic anhydride, dodecanoic anhydride, tetradecanoic anhydride, and hexadecanoic anhydride were purchased from Sigma-Aldrich. 1,2-distearoyl-*sn*-glycero-3-phosphoethanolamine-N-[methoxy(polyethylene glycol)-3000] (ammonium salt) (DP 3000) was purchased from Avanti Polar Lipids. Fluorescent dyes, *i.e.*, Dil, Coumarin 6, Nile red, Cy5.5, and DID, were purchased from Thermo Fisher Scientific. All other chemicals if not otherwise specified were purchased from VWR International and used without further purification. RPMI-1640 medium, McCoy's 5A medium, F-12K medium, EMEM medium, trypsin, fetal bovine serum (FBS), penicillin-streptomycin solution, phosphate-buffered saline (PBS), and water were supplied by Gibco®.

Synthesis of Pt(IV) 1-8

4.0 mL of 30 w/v% H_2O_2 was added dropwise into a 10.0 mL of 10 w/v% cisplatin suspension. The mixture was kept stirring against light at 25°C for 24 h. After recrystallization at 4°C overnight, the product was collected and washed with ice-cold water, ethanol, and diethyl ether, respectively. Then, the residual solvent was removed to give a bright yellow powder of *cis,cis,trans*-[$Pt(NH_3)_2Cl_2(OH)_2$] (yield: 90.3%).[1, 2]
Platinum (Pt) drugs, Pt(IV) **1-8,** were all prepared in a manner analogous to that reported earlier:[3, 4] *cis,cis,trans*-[$Pt(NH_3)_2Cl_2(OH)_2$] (0.6 mmol) was suspended in 8.0 mL of dry DMF and reacted with appropriate anhydride (1.4 mmol). After stirring against light at 50°C for 24 h, the resulting solution was filtered, evaporated to 1.0 mL, and dropwise added to a rapidly stirring volume (40.0 mL) of diethyl ether. Then, the resultant precipitate was collected, washed with acetone and diethyl ether, and dried under vacuum for 24 h.

NMR spectra

^{1}H and ^{13}C NMR spectra of Pt(IV) **1-8** were recorded on a Mercury VX-300 Nuclear Magnetic Resonance (NMR) spectrometer at 400 MHz (Varian, USA) using DMF-d_7 as the solvent and MestReNova software for data analysis. Chemical shifts were internally referenced to solvent signals (^{1}H NMR: DMF at δ = 2.75, 2.92, 8.03 ppm; ^{13}C NMR: DMF at δ = 29.76, 34.89, 163.15 ppm).
Pt(IV) **1**, *cis,cis,trans*-[$Pt(NH_3)_2Cl_2(OOCCH_3)_2$]: Pale yellow powder (yield: 79.2 %); ^{1}H NMR δ = 1.88 (*s*, 6H, C*H*$_3$), 6.65-7.04 (*m*, 6H, N*H*$_3$) ppm; ^{13}C NMR δ = 22.19 (*C*H_3), 178.97 (*C*O) ppm.
Pt(IV) **2**, *cis,cis,trans*-[$Pt(NH_3)_2Cl_2(OOC(CH_2)_2CH_3)_2$]: Off-white powder (yield: 78.6 %); ^{1}H NMR δ = 1.03 (*t*, 6H, C*H*$_3$), 1.66 (*sext*, 4H, C*H*$_2$CH$_3$), 2.35 (*t*, 4H, COC*H*$_2$), 6.82-7.21 (*m*, 6H, N*H*$_3$) ppm; ^{13}C NMR δ = 13.47 (*C*H_3), 19.28 (*C*H_2CH_3), 38.06 (CO*C*H_2), 181.69 (*C*O) ppm.
Pt(IV) **3**, *cis,cis,trans*-[$Pt(NH_3)_2Cl_2(OOC(CH_2)_4CH_3)_2$]: Off-white powder (yield: 77.9 %); ^{1}H NMR δ = 1.02 (*t*, 6H, C*H*$_3$), 1.42 (*m*, 8H, (C*H*$_2$)$_2$), 1.64 (*quint*, 4H, COCH$_2$C*H*$_2$), 2.37 (*t*, 4H, COC*H*$_2$), 6.83-7.21 (*m*, 6H, N*H*$_3$) ppm; ^{13}C NMR δ = 13.72

(*C*H_3), 22.46 (*C*H_2CH$_3$), 25.66 (COCH$_2$*C*H_2), 31.42 (*C*H_2CH$_2$CH$_3$), 36.09 (CO*C*H_2), 181.82 (*C*O) ppm.

Pt(IV) **4**, *cis,cis,trans*-[Pt(NH$_3$)$_2$Cl$_2$(OOC(CH$_2$)$_6$CH$_3$)$_2$]: Off-white powder (yield: 70.0 %); ^{1}H NMR δ = 1.03 (*t*, 6H, C*H*$_3$), 1.41 (*m*, 16H, (C*H*$_2$)$_4$), 1.64 (*quint*, 4H, COCH$_2$C*H*$_2$), 2.38 (*t*, 4H, COC*H*$_2$), 6.84-7.20 (*m*, 6H, N*H*$_3$) ppm; ^{13}C NMR δ = 13.81 (*C*H$_3$), 22.62 (*C*H$_2$CH$_3$), 26.01 (COCH$_2$*C*H$_2$), 29.19 ((*C*H$_2$)$_2$), 31.82 (*C*H$_2$CH$_2$CH$_3$), 36.15 (CO*C*H$_2$), 181.83 (*C*O) ppm.

Pt(IV) **5**, *cis,cis,trans*-[Pt(NH$_3$)$_2$Cl$_2$(OOC(CH$_2$)$_8$CH$_3$)$_2$]: White powder (yield: 68.9 %); ^{1}H NMR δ = 1.03 (*t*, 6H, C*H*$_3$), 1.42 (*m*, 24H, (C*H*$_2$)$_6$), 1.64 (*quint*, 4H, COCH$_2$C*H*$_2$), 2.38 (*t*, 4H, COC*H*$_2$), 6.82-7.21 (*m*, 6H, N*H*$_3$) ppm; ^{13}C NMR δ = 13.83 (*C*H$_3$), 22.65 (*C*H$_2$CH$_3$), 26.02 (COCH$_2$*C*H$_2$), 29.58 ((*C*H$_2$)$_4$), 31.93 (*C*H$_2$CH$_2$CH$_3$), 36.16 (CO*C*H$_2$), 181.63 (*C*O) ppm.

Pt(IV) **6**, *cis,cis,trans*-[Pt(NH$_3$)$_2$Cl$_2$(OOC(CH$_2$)$_{10}$CH$_3$)$_2$]: White powder (yield: 60.1 %); ^{1}H NMR δ = 1.03 (*t*, 6H, C*H*$_3$), 1.43 (*m*, 32H, (C*H*$_2$)$_8$), 1.64 (*quint*, 4H, COCH$_2$C*H*$_2$), 2.38 (*t*, 4H, COC*H*$_2$), 6.82-7.20 (*m*, 6H, N*H*$_3$) ppm; ^{13}C NMR δ = 13.82 (*C*H$_3$), 22.64 (*C*H$_2$CH$_3$), 26.02 (COCH$_2$*C*H$_2$), 29.89 ((*C*H$_2$)$_6$), 31.94 (*C*H$_2$CH$_2$CH$_3$), 36.17 (CO*C*H$_2$), 181.83 (*C*O) ppm.

Pt(IV) **7**, *cis,cis,trans*-[Pt(NH$_3$)$_2$Cl$_2$(OOC(CH$_2$)$_{12}$CH$_3$)$_2$]: White powder (yield: 62.4 %); ^{1}H NMR δ = 1.03 (*t*, 6H, C*H*$_3$), 1.43 (*m*, 40H, (C*H*$_2$)$_{10}$), 1.64 (*quint*, 4H, COCH$_2$C*H*$_2$), 2.38 (*t*, 4H, COC*H*$_2$), 6.84-7.21 (*m*, 6H, N*H*$_3$) ppm; ^{13}C NMR δ = 13.65 (*C*H$_3$), 22.48 (*C*H$_2$CH$_3$), 25.86 (COCH$_2$*C*H$_2$), 29.56 ((*C*H$_2$)$_8$), 31.77 (*C*H$_2$CH$_2$CH$_3$), 36.00 (CO*C*H$_2$), 181.66 (*C*O) ppm.

Pt(IV) **8**, *cis,cis,trans*-[Pt(NH$_3$)$_2$Cl$_2$(OOC(CH$_2$)$_{14}$CH$_3$)$_2$]: White powder (yield: 63.7 %); ^{1}H NMR δ = 1.04 (*t*, 6H, C*H*$_3$), 1.44 (*m*, 48H, (C*H*$_2$)$_{12}$), 1.64 (*quint*, 4H, COCH$_2$C*H*$_2$), 2.38 (*t*, 4H, COC*H*$_2$), 6.88-7.14 (*m*, 6H, N*H*$_3$) ppm; ^{13}C NMR δ = 13.65 (*C*H$_3$), 22.48 (*C*H$_2$CH$_3$), 25.86 (COCH$_2$*C*H$_2$), 29.57 ((*C*H$_2$)$_{10}$), 31.77 (*C*H$_2$CH$_2$CH$_3$), 36.00 (CO*C*H$_2$), 181.65 (*C*O) ppm.

Electrochemistry

Pt(IV) **1-8** were dissolved in DMF:0.1 M aqueous KCl buffered with phosphate to either pH 6.0 or 7.4 = 1:4. Deaeration of solutions was accomplished by passing a stream of argon through the solution for 5 min prior to the measurement and then maintaining a blanket atmosphere of argon over the solution during the measurement. The cyclic voltammogram was recorded at room temperature with a CHI600E Electrochemical Analyzer, using a three-electrode set-up comprising a glassy carbon working electrode, a Pt wire auxiliary electrode, and an Ag/AgCl reference electrode.[5] The potential was corrected using an internal standard of ferrocenium/ferrocene.

Characterization of Pt(IV) NPs

Particle size and zeta potential were recorded on a ZetaPALS Dynamic Light Scattering Detector (DLS, Brookhaven Instruments, USA) at 25°C and a scattering angle of 90°.

Pt loading was determined with an Inductively Coupled Plasma-Mass Spectrometer (ICP-MS, ICP-MS 7900, Agilent Technologies, USA). The most abundant isotopes of

Pt and indium (used as an internal standard) were measured at m/z 195 and 115, respectively.

TEM study

After centrifugation, P**6** NPs were dispersed in either water or 10 mM dithiothreitol (DTT) at room temperature for 24 h, then diluted with water, negatively stained with 1% uranyl acetate and dried under air. Morphology changes of NPs were visualized on a Tecnai G2 Spirit BioTWIN Transmission Electron Microscope (TEM, FEI, USA) at 80 kV.

***In vitro* redox-triggered Pt release**

P**6** NPs were transferred into a Float-A-Lyzer G2 dialysis device (MWCO 100 KDa, Spectrum). Drug release was conducted in PBS (pH 7.4) at 37 °C with stirring at 100 rpm. At designed time points, 0.1 mL of sample solution was withdrawn and the Pt concentration was quantified with an ICP-MS. Equal volumes of fresh PBS were immediately replenished. The same Pt release procedure was carried out in triplicates in the presence of 1 mM and 10 mM DTT, respectively.

Cell culture

A2780 and A2780cis cells were purchased from European Collection of Authenticated Cell Cultures (ECACC). PC-3, MCF7, HCT116, A549, and H460 cells were purchased from American Type Culture Collection (ATCC). Master and working cell banks were generated immediately upon receipt, the third and fourth passages were used for tumor experiments. Cells were tested every three months for potential mycoplasma. Re-authentication of cells was not performed after receipt. All cells were cultured using recommended manufacturer protocols. For example, A2780cis cells established from cisplatin-resistant ovarian carcinoma were grown in RPMI-1640 medium, supplemented with 10% FBS and 1 μM cisplatin. Exponentially growing cultures were maintained at 37 °C under an atmosphere of 5% CO_2 and 90% relative humidity, and grown to 70% confluence before splitting or harvesting.

Cellular uptake

A2780 and A2780cis cells were seeded in 6-well plates (50,000 cells per well) and incubated with 1 mL of RPMI-1640 medium containing 10% FBS for 24 h. Subsequently, cells were exposed to cisplatin, P**6** NPs, or P**6** Soln at different concentrations. At selected time intervals, cells were washed with PBS three-times, and then collected. The protein concentration was measured using the Bicinchoninic Acid Protein Assay Kit (BCA, Pierce, Thermo Fisher Scientific, USA) according to the manufacturer protocol with a Synergy HT Multi-Mode Microplate Reader (BioTek Instruments, USA) and the Pt concentration was determined with an ICP-MS.

Intracellular disintegration

A2780 and A2780cis cells were seeded in 35 mm sterile glass bottom culture dishes (20,000 cells per dish) and incubated with 1 mL of RPMI-1640 medium containing 10% FBS for 24 h. Coumarin 6 (Ex/Em = 410/520 nm) and Nile red (Ex/Em = 530/590 nm) were co-loaded as the FRET (Förster Resonance Energy Transfer) pair to interrogate intracellular behaviors of P**6** NPs. Subsequently, cells were treated with Opti-MEM (Thermo Fisher Scientific, USA) for 30 min prior to incubation with Coumarin 6 and Nile red-P**6** NPs. At predetermined time points, cells were washed with PBS three-times and imaged under an FV1200 Confocal Laser Scanning Microscope (CLSM, Olympus, Japan) (Ex = 410 nm, Em = 520 and 590 nm).

To investigate the effect of intracellular GSH on NP disintegration, A2780 and A2780cis cells were pretreated with 50 μM N-ethylmaleimide (NEM) for 1 h to consume sulfhydryl, followed with all other procedure carried out as described above.

Intracellular GSH and GSSH assay

A2780 and A2780cis cells were seeded in dishes (1,000,000 cells per dish) and incubated with 5 mL of RPMI-1640 medium containing 10% FBS for 24 h. After incubation with cisplatin, P**6** NPs, or P**6** Soln at different concentrations for 24 h, cells were collected, homogenized, and centrifuged. The supernatant was used for reduced (GSH) and oxidized (GSSG) glutathione assay according to the manufacturer protocol (Glutathione Fluorometric Assay Kit, BioVision, USA) with a Microplate Reader.

Subcellular fractionation

A2780 and A2780cis cells were seeded in dishes (1,000,000 cells per dish) and incubated with 5 mL of RPMI-1640 medium containing 10% FBS for 24 h. After incubation with cisplatin, P**6** NPs, or P**6** Soln at 100 μM for 24 h, cells were collected and subcellular fractions were isolated according to the manufacturer protocol (ProteoExtract Subcellular Proteome Extraction Kit, Merck KGaA, Germany). The total protein concentration was measured using a BCA Kit with a Microplate Reader and Pt concentration in each subcellular fraction was quantified with an ICP-MS.

Pt-DNA adduct

A2780 and A2780cis cells were seeded in dishes (1,000,000 cells per dish) and incubated with 5 mL of RPMI-1640 medium containing 10% FBS for 24 h. After incubation with cisplatin, P**6** NPs, or P**6** Soln at 100 μM for 24 h, cells were incubated with fresh medium for another 12 h, then collected and DNA was isolated according to the manufacturer protocol (DNAzol Reagent, Thermo Fisher Scientific, USA). The DNA concentration was measured with a NanoDrop 2000 (Thermo Fisher Scientific, USA) and the Pt concentration was determined with an ICP-MS.

***In vitro* proliferation**

A2780, A2780cis, PC-3, MCF7, HCT116, A549, and H460 cells were seeded in 96-well plates (5,000 cells per well) and incubated with 100 μL of corresponding medium containing 10% FBS for 24 h. Thereafter, cells were treated with cisplatin, P**6** NPs, or P**6** Soln at different concentrations. At predetermined intervals, cytotoxicity was evaluated according to the manufacturer protocol (AlamarBlue Cell Viability Assay, Thermo Fisher Scientific, USA) with a Microplate Reader.

Live/dead cell viability

A2780 and A2780cis cells were seeded in 35 mm sterile glass bottom culture dishes (20,000 cells per dish) and incubated with 1 mL of RPMI-1640 medium containing 10% FBS for 24 h. Thereafter, cisplatin, P**6** NPs, P**6** Soln, or DP 3000 at 25 μM were added. After 24 h, cells were washed with PBS three-times and treated according to the manufacturer protocol (Live/dead™ Viability/Cytotoxicity Kit, Thermo Fisher Scientific, USA) under a CLSM. The amount of DP 3000 incubated was equal in weight to that of P**6** NPs.

***In vitro* apoptosis**

A2780 and A2780cis cells were seeded in 6-well plates (50,000 cells per well) and incubated with 1 mL of RPMI-1640 medium containing 10% FBS for 24 h. Thereafter, cells were treated with cisplatin, P**6** NPs, or P**6** Soln at different concentrations. After 24 h, apoptosis was evaluated according to the manufacturer protocol (Dead Cell Apoptosis Kit with Annexin V Alexa-Fluor 488 and Propidium Iodide, Thermo Fisher Scientific, USA) with a Flow Cytometry (FACSAriaTM III, BD, USA).

Nuclear staining

A2780 and A2780cis cells were seeded in 35 mm sterile glass bottom culture dishes (20,000 cells per dish) and incubated with 1 mL of RPMI-1640 medium containing 10% FBS for 24 h. Thereafter, cisplatin, P**6** NPs, P**6** Soln, or DP 3000 at 25 μM was added. After 24 h, cells were washed with PBS three-times and treated according to the manufacturer protocol (NucBlue Live ReadyProbes Reagent, Thermo Fisher Scientific, USA) under a CLSM.

Animals and xenograft tumor model

Healthy BALB/c mice (5-6 weeks old) and athymic nude mice (4-5 weeks old) were purchased from Charles River Laboratories. All the animals were treated in accordance with National Institutes of Health animal care guidelines and in strict pathogen-free conditions in the animal facility of Brigham and Women's Hospital. The animal protocol was approved by the Institutional Animal Care and Use Committees (Harvard Medical School).

The xenograft tumor model was generated by subcutaneously injecting cell suspension (2,000,000 cells in 100 μL of medium and 100 μL of Matrigel) into the back or flank of athymic nude mouse. As the volume of xenograft tumor reached ~100 mm^3, the mice were used for *in vivo* experiments.

Pharmacokinetic design and analysis

BALB/c mice were randomly assigned to three groups (Male, n = 3) and given an intravenous injection of *(I)* cisplatin, *(II)* P**6** NPs, or *(III)* P**6** Soln at 4.55 mg Pt/kg. At predetermined time intervals, blood was withdrawn from retro-orbital plexus, heparinized, and centrifuged. The supernatant was separated and stored at -80 °C until analysis.

For the analysis of plasma samples, 20 μL of plasma was lyophilized. The dry residue was suspended in 40 μL of HNO_3, boiled for 1 h, diluted with 60 μL of 0.1 M HCl, and then analyzed with an ICP-MS.

Pharmacokinetic profiles were calculated using a Phoenix WinNonlin 6.3 Program (Pharsight Cooperation, USA) and following parameters were obtained: the area under the plasma concentration-time curve from time zero to time infinity ($AUC_{0\rightarrow inf}$), the area under the plasma concentration-moment curve from time zero to time infinity ($AUMC_{0\rightarrow inf}$), total body clearance (CL), volume of distribution at steady state (V_{ss}), mean residence time from time zero to time infinity ($MRT_{0\rightarrow inf}$), hybrid constants (A, α, B, β), apparent plasma half-life of distribution and elimination phases ($t_{1/2\alpha}$, $t_{1/2\beta}$), and first-order rate constants (k_{10}, k_{12}, k_{21}).

Biodistribution

A2780cis tumor-bearing athymic nude mice were randomly assigned to three groups (Female, n = 3) and given an intravenous injection of *(I)* cisplatin, *(II)* P**6** NPs, or *(III)* P**6** Soln at 4.55 mg Pt/kg. At predetermined time intervals, mice were sacrificed, and their plasma, organs (heart, liver, spleen, lung, kidney), and tumors were collected.

For the analysis of tissue samples, entire tissue was lyophilized. The dry residue was weighted, digested with HNO_3 (500 μL/200 mg tissue) overnight at room temperature, and boiled for 3-5 min. 30 w/v% H_2O_2 was added in a volume equal to HNO_3. The mixture was vortexed for 5 min, boiled for another 3-5 min, then analyzed with an ICP-MS.

The analysis of plasma samples was the same as described above.

***In vivo* survival analysis**

A2780 and A2780cis tumor-bearing athymic nude mice were randomly assigned to five groups (Female, n = 5) and intravenously injected with *(I)* PBS, *(II)* cisplatin, *(III)* P**6** NPs, *(IV)* P**6** Soln, or *(V)* DP 3000 at 4.0 mg Pt/kg. The mice were injected at seven-day intervals over a period of 63 days, with the first injection day designated day 0.

Survival time was monitored every day, and mice were euthanized as they became moribund. Time to death (or euthanization) was completed using the Kaplan-Meier estimate of survival time, stratified by treatment group. Equality of survival was determined using the log-rank test.

Western blot

A2780 and A2780cis tumor-bearing athymic nude mice were randomly assigned to five groups (Female, n = 5) and intravenously injected with *(I)* PBS, *(II)* cisplatin, *(III)* P**6** NPs, *(IV)* P**6** Soln, or *(V)* DP 3000 at 4.0 mg Pt/kg. The mice were injected four-times at seven-day intervals. After that, mice were sacrificed, and their tumors were quickly collected and immediately stored in liquid nitrogen. The blots were conducted with the three of five tumor tissues in each group randomly

Proteins in tumors were extracted with Radioimmunoprecipitation Assay Lysis Buffer (Cell Signaling, USA), supplemented with Protease/Phosphatase Inhibitor Cocktail (Cell Signaling, USA) and Phenylmethanesulfonyl fluoride (PMSF, Cell Signaling, USA). Equal amounts of these proteins, as determined using the BCA Kit, were added to the SDS-PAGE gel and separated by electrophoresis. After transferring proteins from the gel to polyvinylidene difluoride (PVDF) membrane, the membrane was blocked with 3% BSA in TBST (50 mM Tris-HCl pH 7.4, 150 mM NaCl, 0.1% Tween 20), then incubated with primary antibodies (p53, Caspase 3, PARP, or Cleaved PARP, Cell Signaling, USA) and β-actin rabbit antibodies (Cell Signaling, USA). Subsequently, blots were incubated with HRP-conjugated secondary antibodies (Goat anti-rabbit IgG, Cell Signaling, USA) and an Enhanced Chemiluminescence Detection System (ECL, Pierce, Thermo Fisher Scientific, USA) before finally being exposed on blue autoradiography films (Amersham Biosciences, USA).

Blood biochemistry

A2780 and A2780cis tumor-bearing athymic nude mice were randomly assigned to five groups (Female, n = 5) and intravenously injected with *(I)* PBS, *(II)* cisplatin, *(III)* P**6** NPs, *(IV)* P**6** Soln, or *(V)* DP 3000 at 4.0 mg Pt/kg. The mice were injected four-times at seven-day intervals. After that, blood was collected by cardiac puncture, and serum was separated for measuring alanine aminotransferase (ALT), aspartate aminotransferase (AST), alkaline phosphatase (ALP), blood urea nitrogen (BUN), and serum creatinine (Cre) with an Automatic Biochemical Analyzer (UniCel DxC 800 Synchron Clinical System, Beckman Coulter, USA).

ECL and ELISA assay

BALB/c mice were randomly assigned to five groups (Female, n = 5) and intravenously injected with *(I)* PBS, *(II)* cisplatin, *(III)* P**6** NPs, *(IV)* P**6** Soln, or *(V)* DP 3000 at 4.0 mg Pt/kg. After 24 and 72 h, mice were sacrificed, and their kidneys were quickly collected and homogenized in PBS containing 0.05% Tween 20. Electrochemilumenescence Assay (ECL) for Interleukin-1β (IL-1β) and Interleukin-18 (IL-18) in whole-kidney homogenates was performed as described previously in detail.[6, 7] Enzyme-linked Immunosorbent Assay (ELISA) for Interleukin-6 (IL-6) and Tumor Necrosis Factor-α (TNF-α) in whole-kidney homogenates was performed using mouse ELISA sets (R&D Systems, USA) according to manufacturer protocols.

Hemolysis

Erythrocytes, collected from BALB/c mice, were diluted with PBS to 2 v/v%. Cisplatin, P**6** NPs, P**6** Soln, DP 3000, and Tween 80 were dispersed in erythrocyte suspension at gradient concentrations and incubated at 37 °C for 3 h, then centrifuged at 1500 rpm for 15 min. The supernatant was measured with a Microplate Reader at 541 nm, and hemolysis rate was determined using the following relationship: Hemolysis rate (%) = $(A_{sample}-A_0)/(A_{100}-A_0) \times 100$, where A_{sample} is the absorbance of the sample, A_{100} is the absorbance of lysed erythrocytes in water (positive control), and A_0 is the absorbance of 0% hemolysis in PBS (negative control).

Statistical analysis

All the experiments were repeated at least three-times and results were expressed as the mean ± standard deviation (SD) unless otherwise noticed. All statistical analyses were performed using a GraphPad Prism 7.0 software (GraphPad Software, USA). One-way analysis of variance (ANOVA) and Tukey post-hoc test were used for multiple comparisons. Survival benefit was determined using a log-rank test. Statistical significance was set at * $p < 0.05$, ** $p < 0.01$, and *** $p < 0.001$. No statistical methods were used to predetermine the sample size of the experiments.

References

1. Ling, X.; Shen, Y.; Sun, R. N.; Zhang, M. Z.; Li, C.; Mao, J. Y.; Xing, J.; Sun, C. M.; Tu, J. S., Tumor-Targeting Delivery of Hyaluronic Acid-Platinum(Iv) Nanoconjugate to Reduce Toxicity and Improve Survival. *Polym. Chem.* **2015,** *6*, 1541-1552.
2. Ling, X.; Zhao, C. Y.; Huang, L. P.; Wang, Q. Y.; Tu, J. S.; Shen, Y.; Sun, C. M., Synthesis and Characterization of Hyaluronic Acid-Platinum(Iv) Nanoconjugate with Enhanced Antitumor Response and Reduced Adverse Effects. *RSC Adv.* **2015,** *5*, 81668-81681.
3. Zanellato, I.; Bonarrigo, I.; Colangelo, D.; Gabano, E.; Ravera, M.; Alessio, M.; Osella, D., Biological Activity of a Series of Cisplatin-Based Aliphatic Bis(Carboxylato) Pt(Iv) Prodrugs: How Long the Organic Chain Should Be? *J. Inorg. Biochem.* **2014,** *140*, 219-227.
4. Johnstone, T. C.; Lippard, S. J., The Effect of Ligand Lipophilicity on the Nanoparticle Encapsulation of Pt(Iv) Prodrugs. *Inorg. Chem.* **2013,** *52*, 9915-9920.
5. Feazell, R. P.; Nakayama-Ratchford, N.; Dai, H.; Lippard, S. J., Soluble Single-Walled Carbon Nanotubes as Longboat Delivery Systems for Platinum(Iv) Anticancer Drug Design. *J. Am. Chem. Soc.* **2007,** *129*, 8438-8439.
6. Wang, W.; Faubel, S.; Ljubanovic, D.; Mitra, A.; Falk, S. A.; Kim, J.; Tao, Y.; Soloviev, A.; Reznikov, L. L.; Dinarello, C. A.; Schrier, R. W.; Edelstein, C. L., Endotoxemic Acute Renal Failure Is Attenuated in Caspase-1-Deficient Mice. *Am. J. Physiol.: Regul. Physiol.* **2005,** *288*, 997-1004.
7. Faubel, S.; Lewis, E. C.; Reznikov, L.; Ljubanovic, D.; Hoke, T. S.; Somerset, H.; Oh, D. J.; Lu, L.; Klein, C. L.; Dinarello, C. A.; Edelstein, C. L., Cisplatin-Induced Acute Renal Failure Is Associated with an Increase in the Cytokines Interleukin

(Il)-1beta, Il-18, Il-6, and Neutrophil Infiltration in the Kidney. *J. Pharmacol. Exp. Ther.* **2007,** *322,* 8-15.

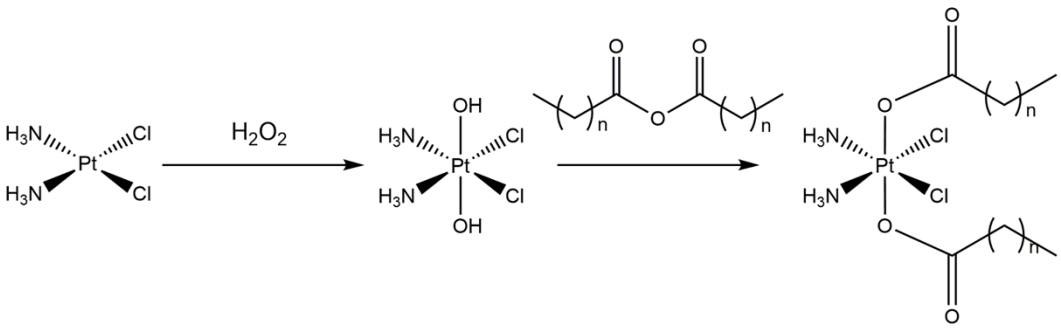

n = 0, 2, 4, 6, 8, 10, 12, 14

Figure S1. Synthetic routes of Pt(IV) **1-8**.

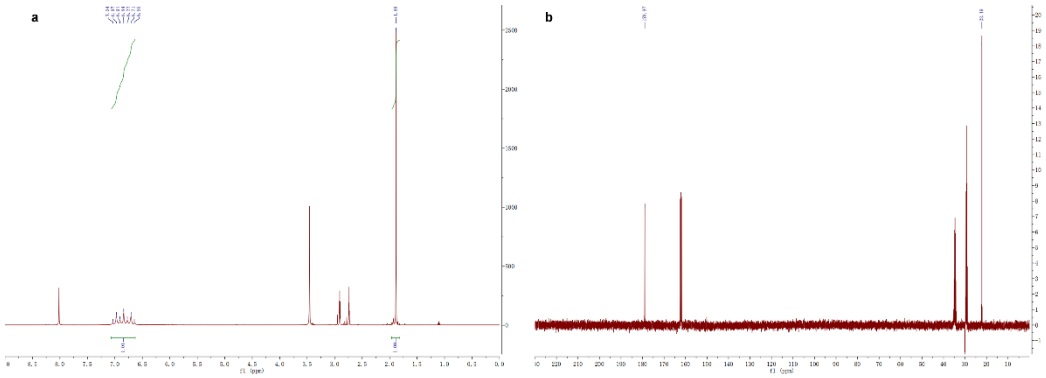

Figure S2. (**a**) ^{1}H and (**b**) ^{13}C NMR spectra of Pt(IV) **1**, *cis*,*cis*,*trans*-$[Pt(NH_3)_2Cl_2(OOCCH_3)_2]$.

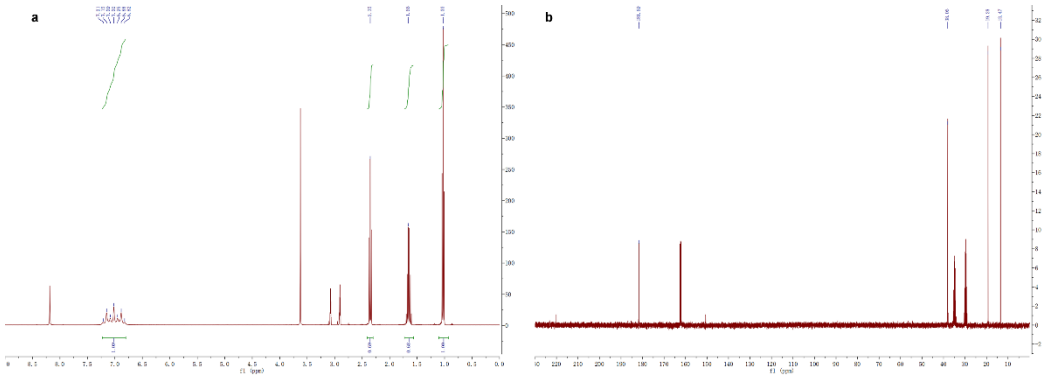

Figure S3. (**a**) ^{1}H and (**b**) ^{13}C NMR spectra of Pt(IV) **2**, *cis*,*cis*,*trans*-$[Pt(NH_3)_2Cl_2(OOC(CH_2)_2CH_3)_2]$.

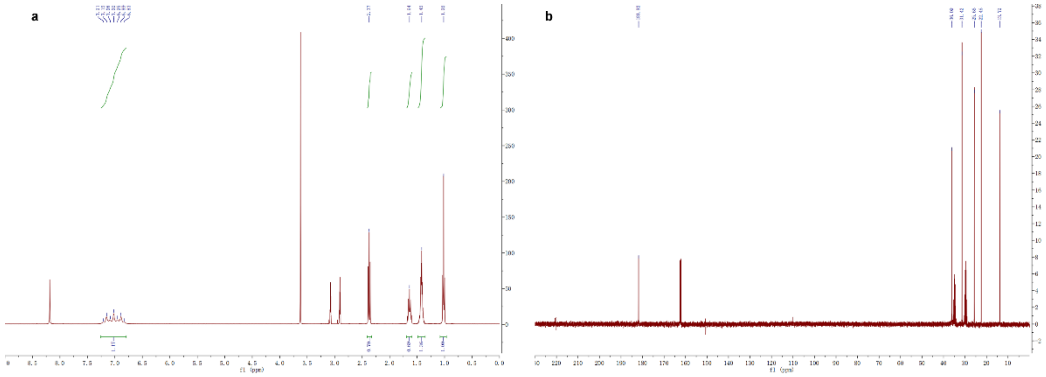

Figure S4. (**a**) ^{1}H and (**b**) ^{13}C NMR spectra of Pt(IV) **3**, *cis,cis,trans*-$[Pt(NH_3)_2Cl_2(OOC(CH_2)_4CH_3)_2]$.

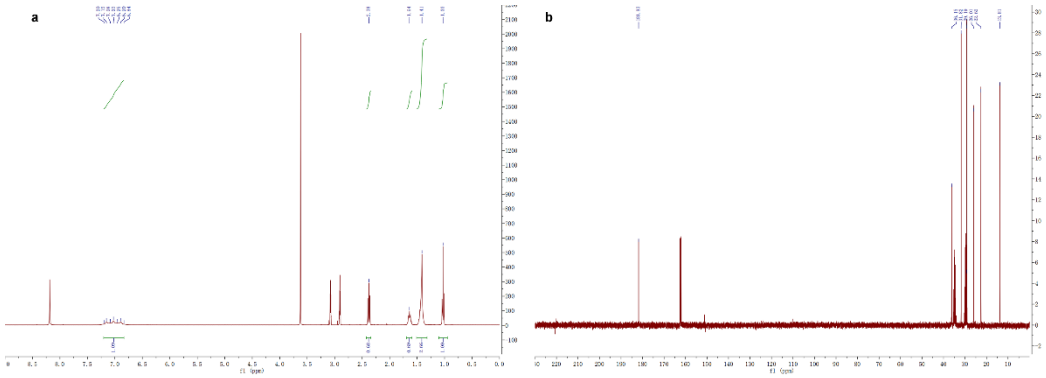

Figure S5. (**a**) ^{1}H and (**b**) ^{13}C NMR spectra of Pt(IV) **4**, *cis,cis,trans*-$[Pt(NH_3)_2Cl_2(OOC(CH_2)_6CH_3)_2]$.

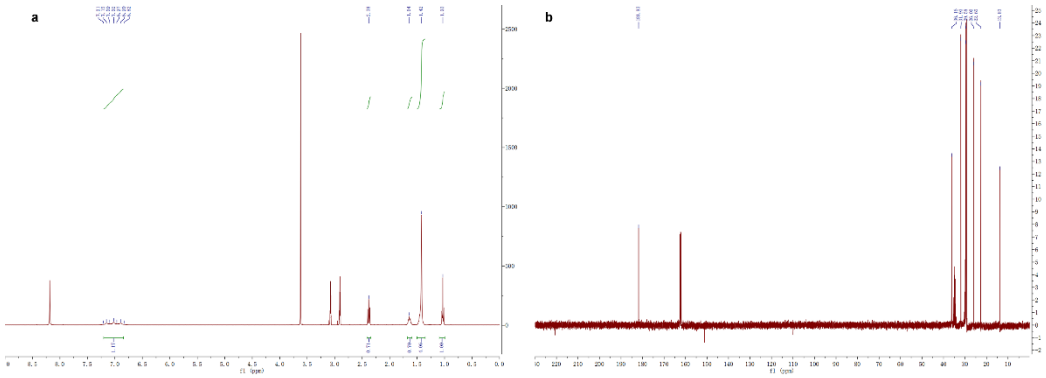

Figure S6. (**a**) ^{1}H and (**b**) ^{13}C NMR spectra of Pt(IV) **5**, *cis,cis,trans*-$[Pt(NH_3)_2Cl_2(OOC(CH_2)_8CH_3)_2]$.

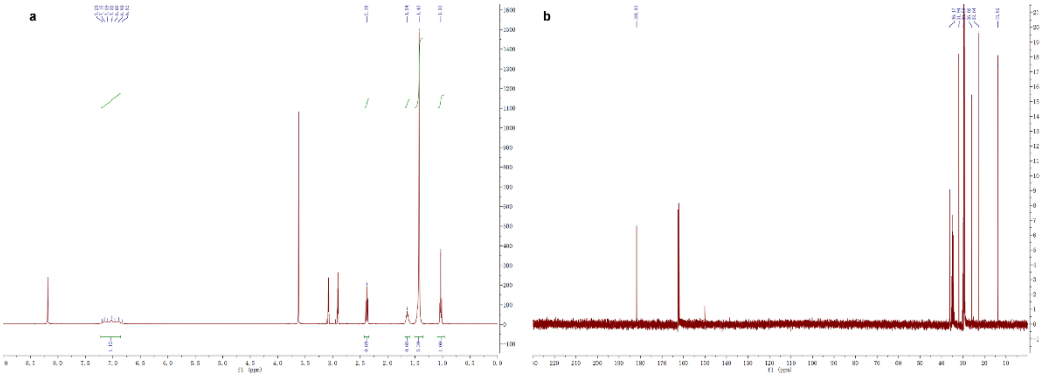

Figure S7. (**a**) ^{1}H and (**b**) ^{13}C NMR spectra of Pt(IV) **6**, *cis*,*cis*,*trans*-[$Pt(NH_3)_2Cl_2(OOC(CH_2)_{10}CH_3)_2$].

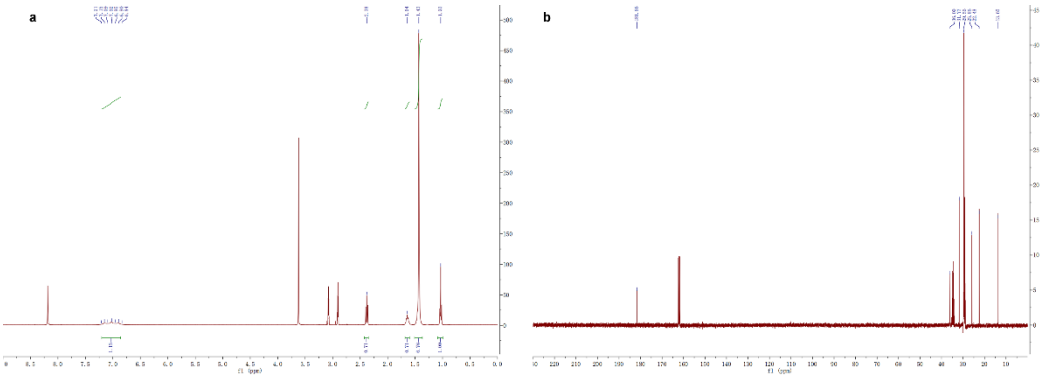

Figure S8. (**a**) ^{1}H and (**b**) ^{13}C NMR spectra of Pt(IV) **7**, *cis*,*cis*,*trans*-[$Pt(NH_3)_2Cl_2(OOC(CH_2)_{12}CH_3)_2$].

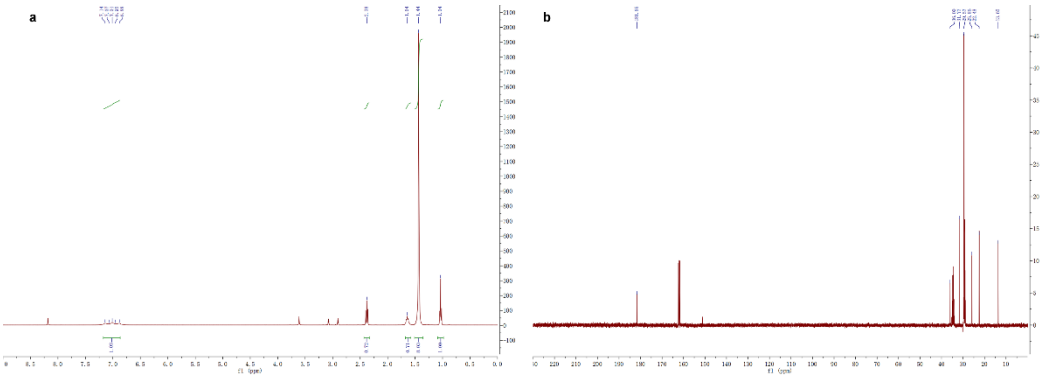

Figure S9. (**a**) ^{1}H and (**b**) ^{13}C NMR spectra of Pt(IV) **8**, *cis*,*cis*,*trans*-[$Pt(NH_3)_2Cl_2(OOC(CH_2)_{14}CH_3)_2$].

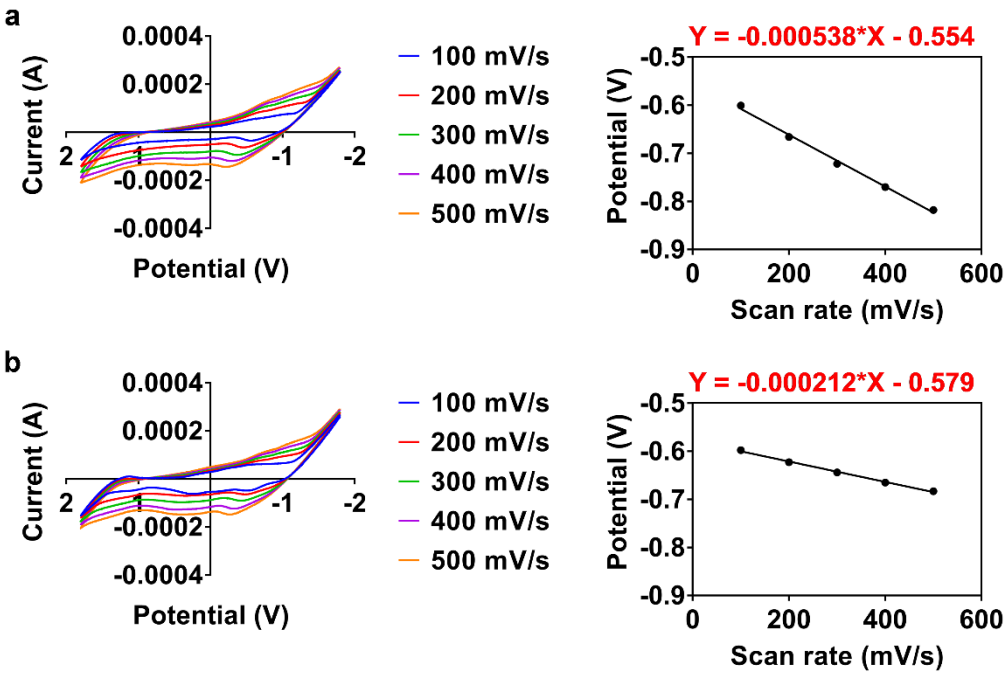

Figure S10. Cyclic voltammograms of Pt(IV) **1** taken at pH (**a**) 6.0 and (**b**) 7.4 with varied scan rates. Plots of reduction peak potential maxima from voltammograms as a function of scan rates.

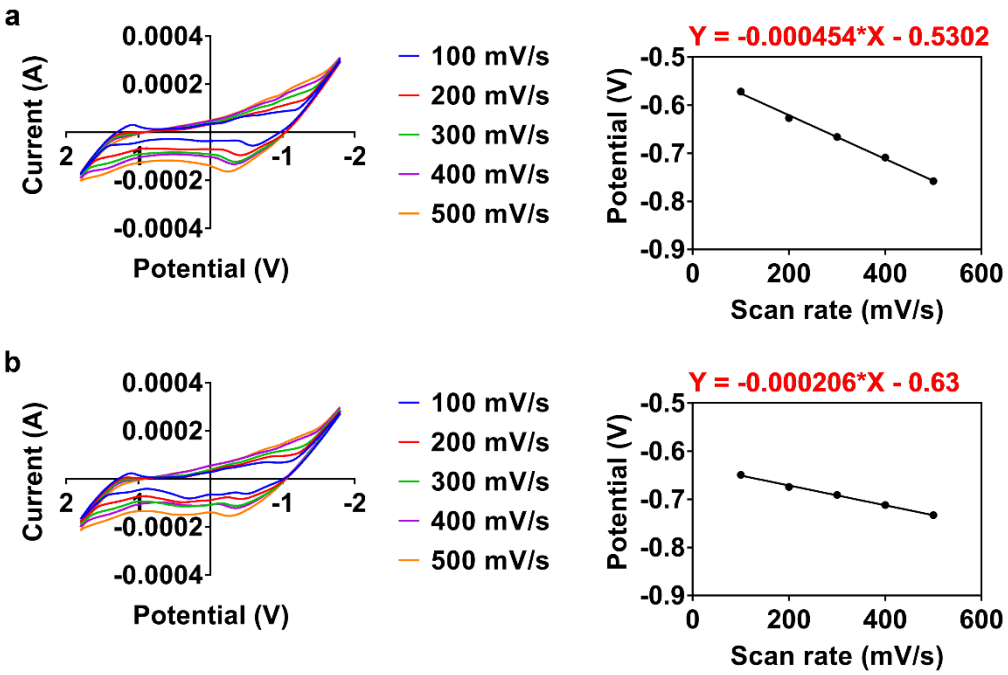

Figure S11. Cyclic voltammograms of Pt(IV) **2** taken at pH (**a**) 6.0 and (**b**) 7.4 with varied scan rates. Plots of reduction peak potential maxima from voltammograms as a function of scan rates.

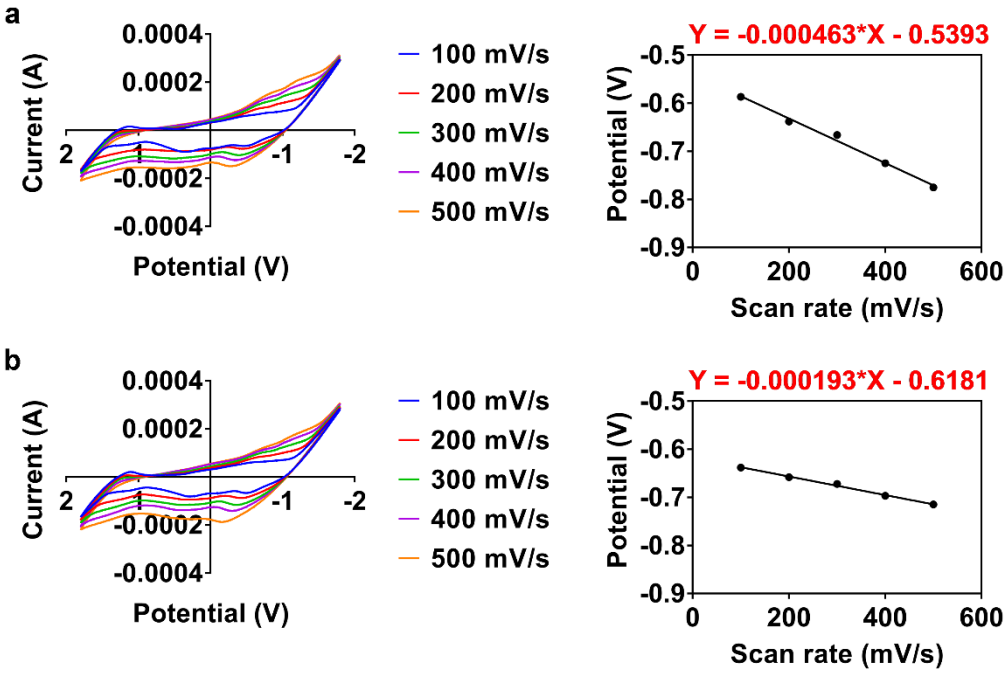

Figure S12. Cyclic voltammograms of Pt(IV) **3** taken at pH (**a**) 6.0 and (**b**) 7.4 with varied scan rates. Plots of reduction peak potential maxima from voltammograms as a function of scan rates.

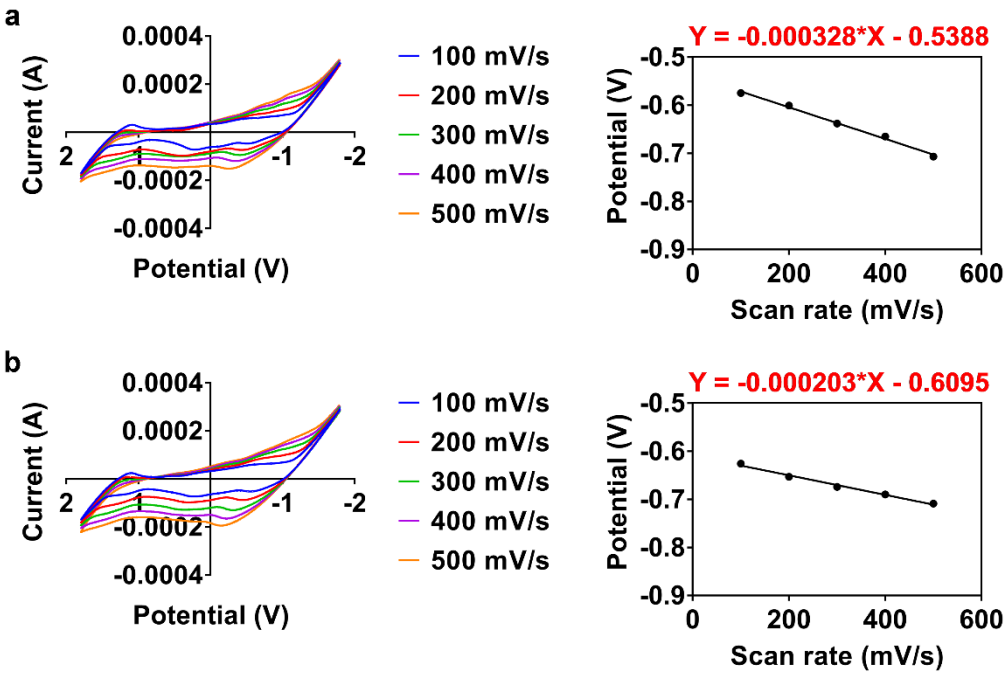

Figure S13. Cyclic voltammograms of Pt(IV) **4** taken at pH (**a**) 6.0 and (**b**) 7.4 with varied scan rates. Plots of reduction peak potential maxima from voltammograms as a function of scan rates.

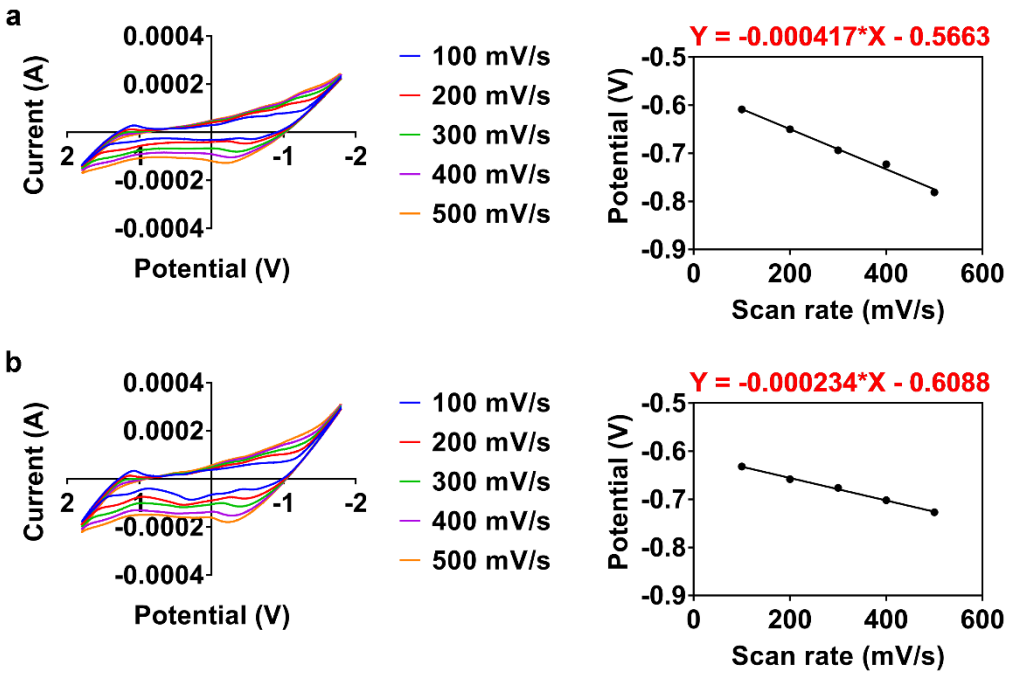

Figure S14. Cyclic voltammograms of Pt(IV) **5** taken at pH (**a**) 6.0 and (**b**) 7.4 with varied scan rates. Plots of reduction peak potential maxima from voltammograms as a function of scan rates.

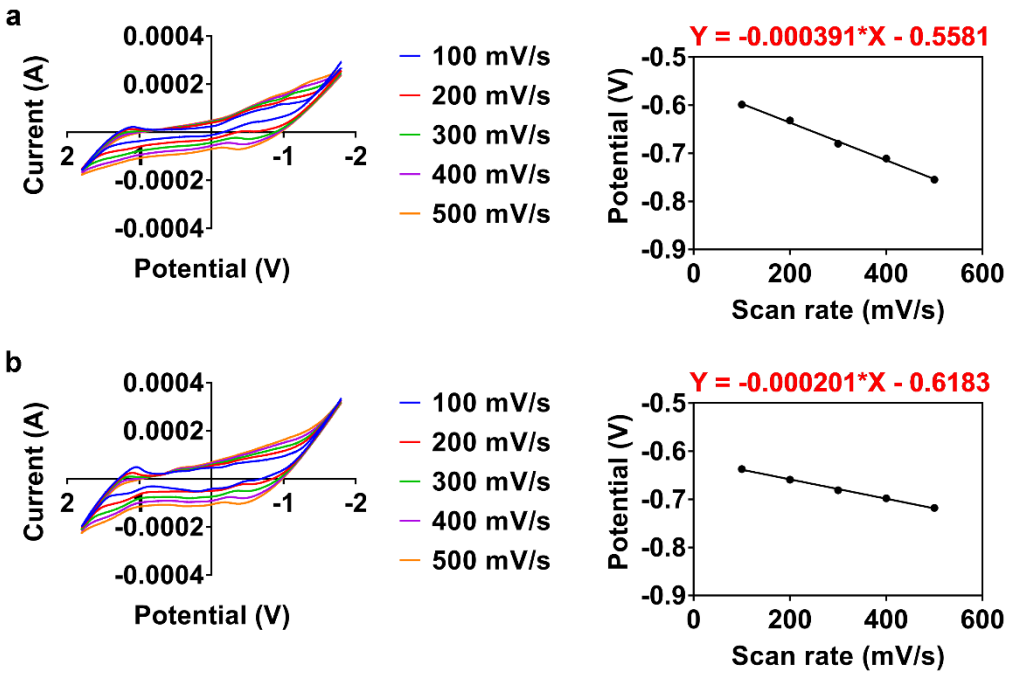

Figure S15. Cyclic voltammograms of Pt(IV) **6** taken at pH (**a**) 6.0 and (**b**) 7.4 with varied scan rates. Plots of reduction peak potential maxima from voltammograms as a function of scan rates.

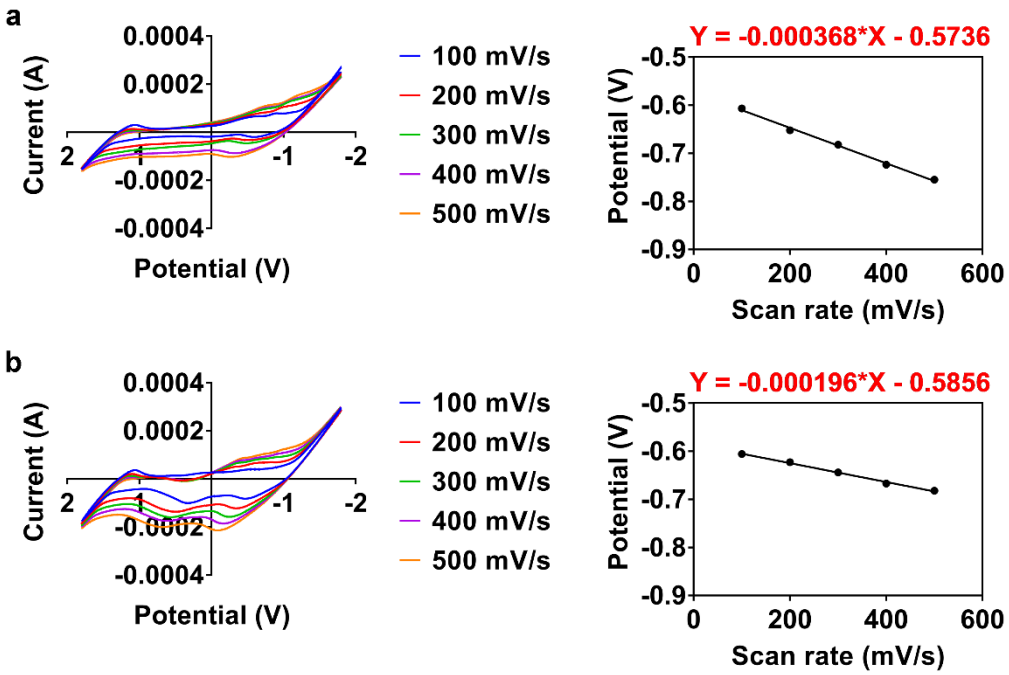

Figure S16. Cyclic voltammograms of Pt(IV) **7** taken at pH (**a**) 6.0 and (**b**) 7.4 with varied scan rates. Plots of reduction peak potential maxima from voltammograms as a function of scan rates.

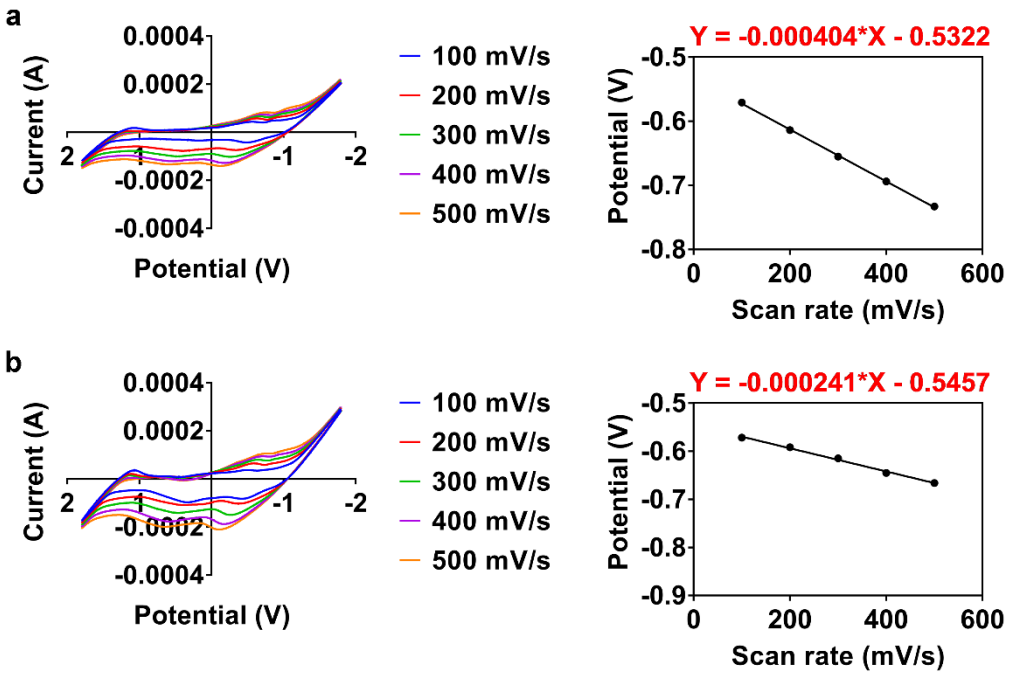

Figure S17. Cyclic voltammograms of Pt(IV) **8** taken at pH (**a**) 6.0 and (**b**) 7.4 with varied scan rates. Plots of reduction peak potential maxima from voltammograms as a function of scan rates.

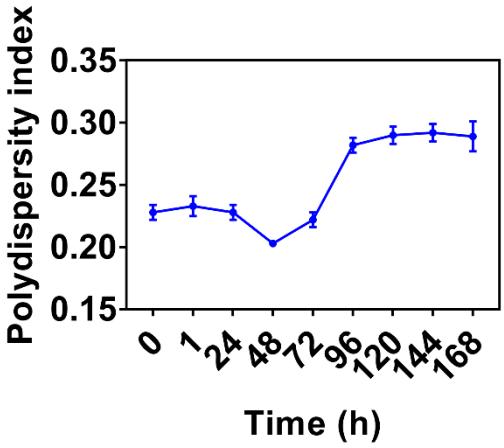

Figure S18. Polydispersity index change of P**6** NPs monitored over the course of one week.

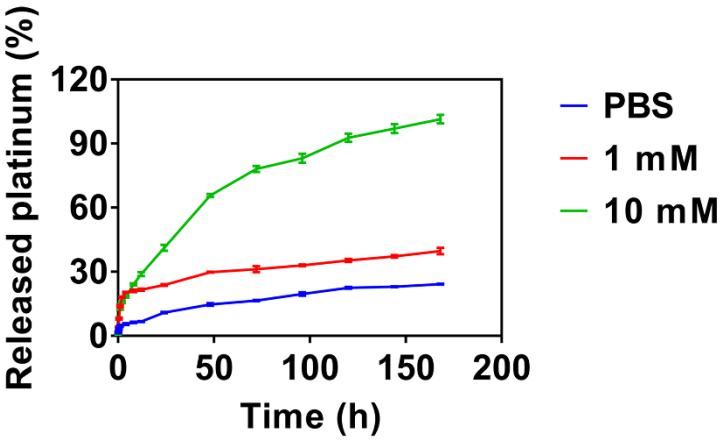

Figure S19. Pt release profiles of P**6** NPs under 0, 1, and 10 mM DTT buffered with phosphate.

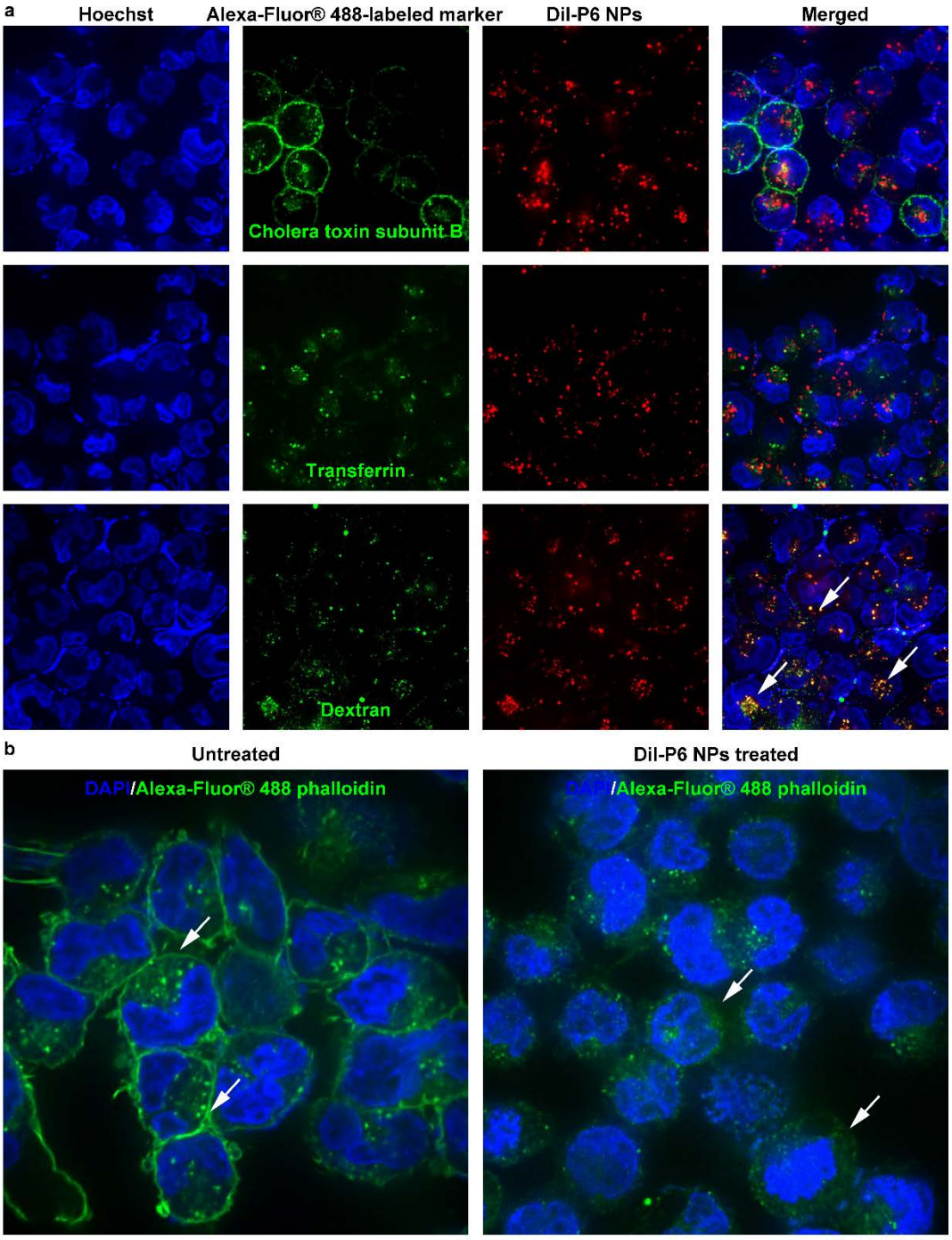

Figure S20. (**a**) DiI-P**6** NPs were incubated with A2780 cells in the presence of Alexa-Fluor 488-labeled markers of various endocytic pathways. NPs co-localized with dextran, a fluid phase marker known to enter cells *via* macropinocytosis (white arrows). (**b**) Alexa-Fluor 488-labeled actin fibers revealed membrane ruffling and actin rearrangement (white arrows), hallmarks of uptake by macropinocytosis.

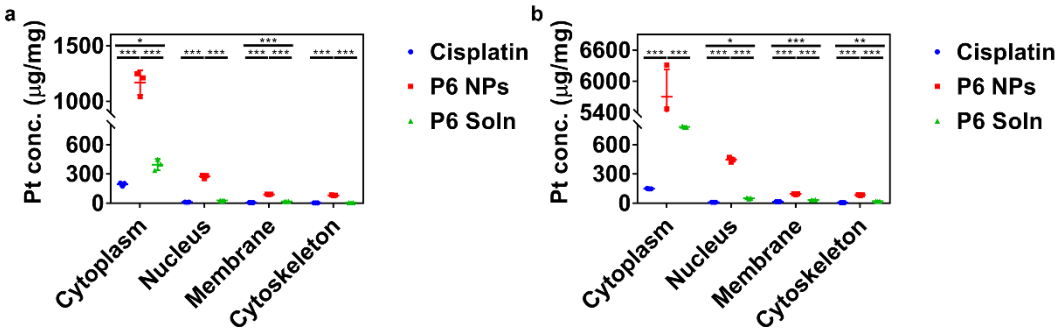

Figure S21. Subcellular distribution of cisplatin, P**6** NPs, or P**6** Soln in (**a**) A2780 and (**b**) A2780cis cells.

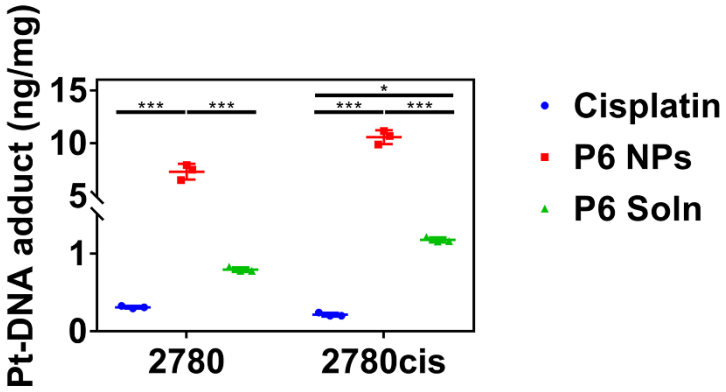

Figure S22. Pt-DNA adducts in A2780 and A2780cis cells treated with cisplatin, P**6** NPs, or P**6** Soln.

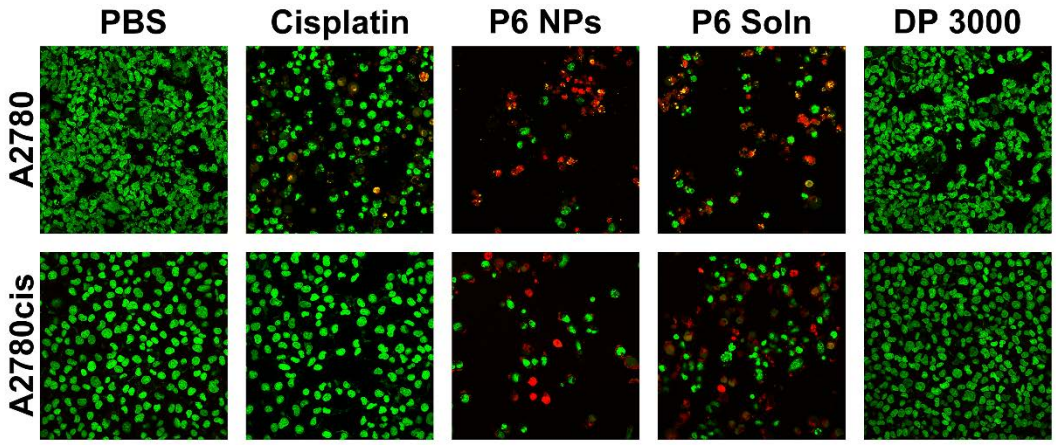

Figure S23. Two-color cellular staining for viability of A2780 and A2780cis cells incubated with PBS, cisplatin, P6 NPs, P6 Soln, or DP 3000. Images were taken under 40× objective.

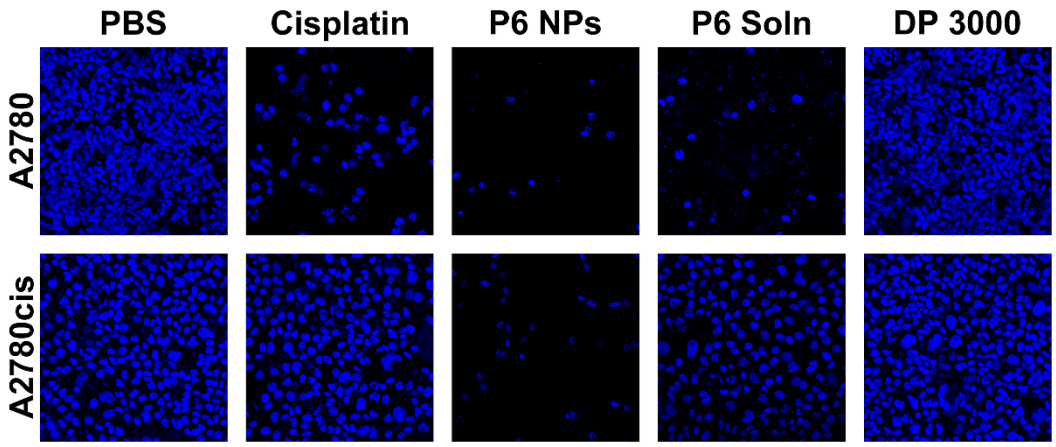

Figure S24. Nuclear staining for apoptosis of A2780 and A2780cis cells incubated with PBS, cisplatin, P**6** NPs, P**6** Soln, or DP 3000. Images were taken under 40× objective.

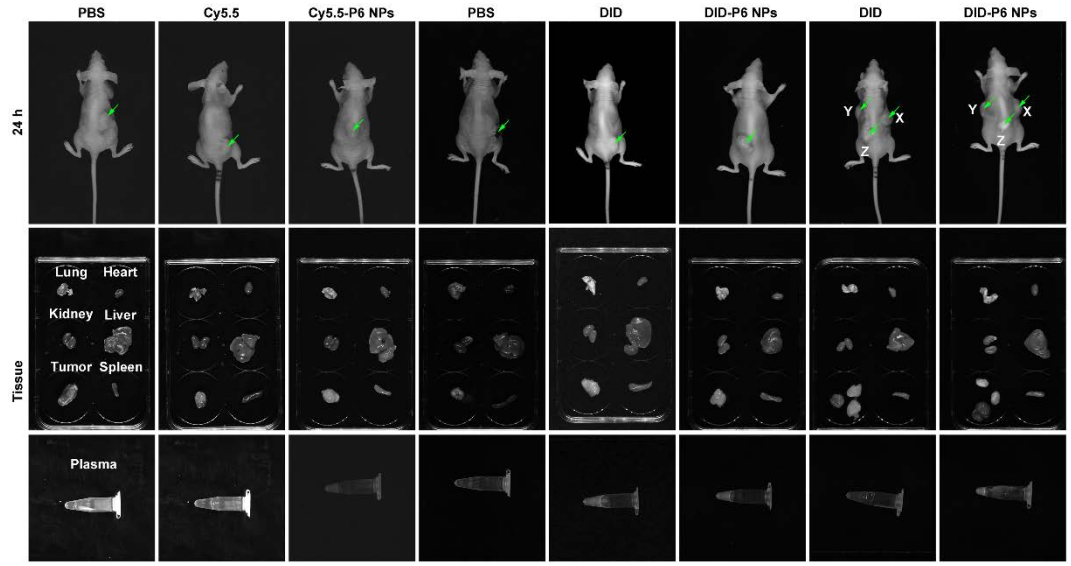

Figure S25. Whole-body images of single or multiple tumor-bearing athymic nude mice and *ex vivo* images of their plasma, organs, and tumors captured using the Maestro 2 *In vivo* imaging system.

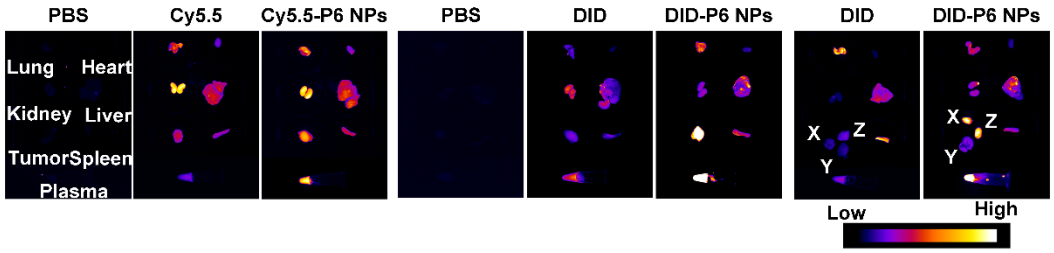

Figure S26. *Ex vivo* fluorescence images of plasma, organs, and tumors captured using the Maestro 2 *In vivo* imaging system.

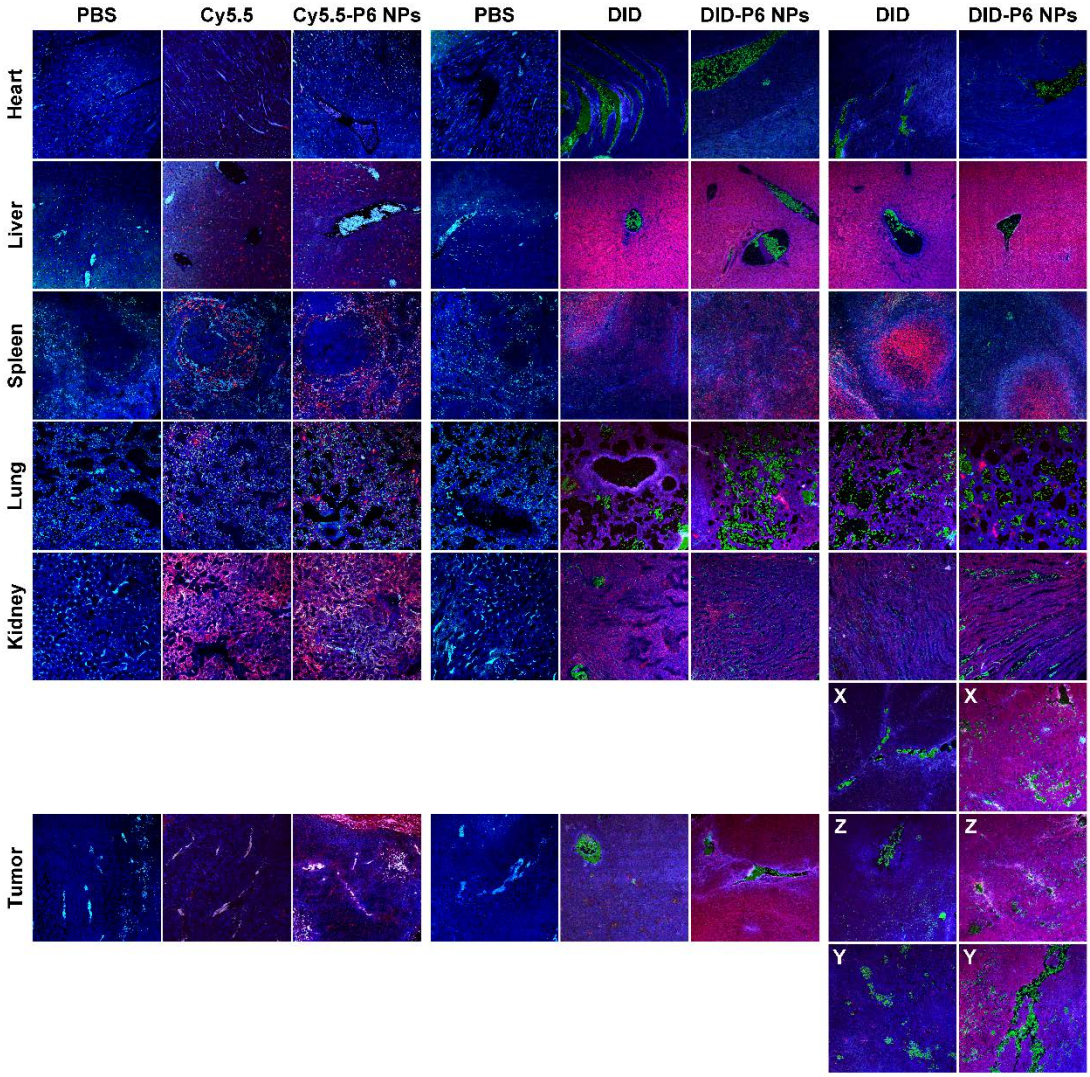

Figure S27. The co-localization of dye or dye-loaded NPs (red) in organs and tumors with nuclei stained with Hoechst 33342 (blue) and microvessels stained with anti-CD31 antibodies (green). Images were taken under 20× objective.

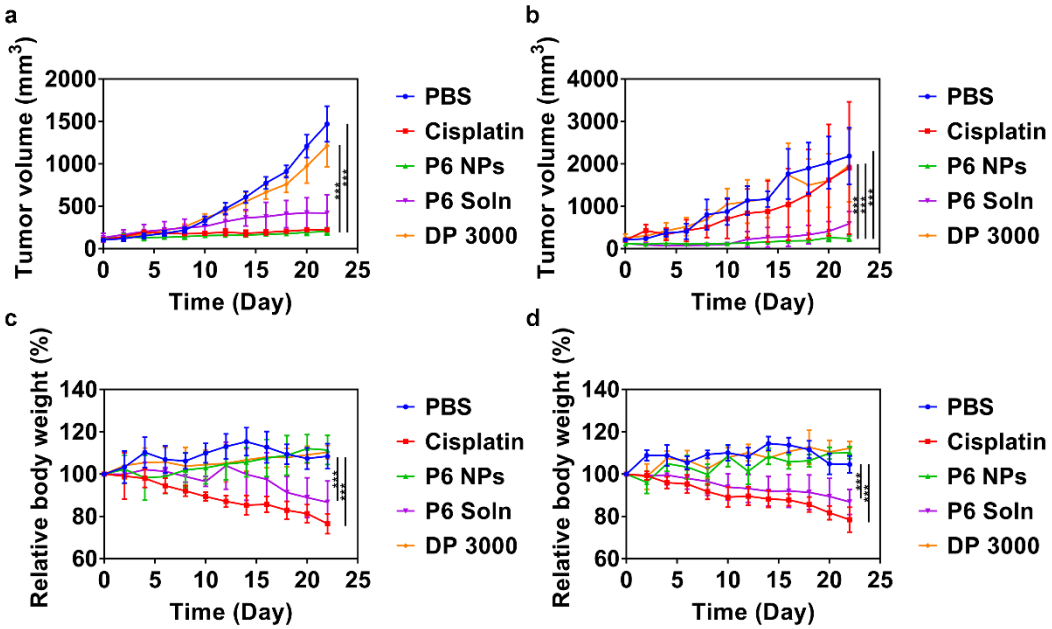

Figure S28. (**a, c**) Tumor-size and (**b, d**) body-weight changes of (**a, b**) A2780 or (**c, d**) A2780cis tumor-bearing athymic nude mice during chemotherapy (n = 5).

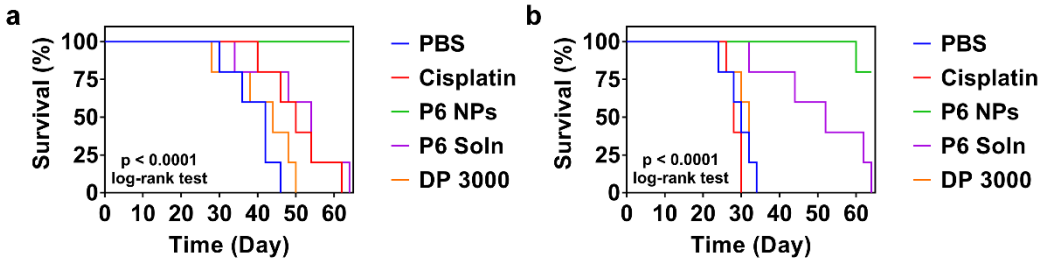

Figure S29. Kaplan-Meier survival curves of (**a**) A2780 and (**b**) A2780cis tumor-bearing athymic nude mice injected once weekly with PBS, cisplatin, P**6** NPs, P**6** Soln, or DP 3000 (n = 5).

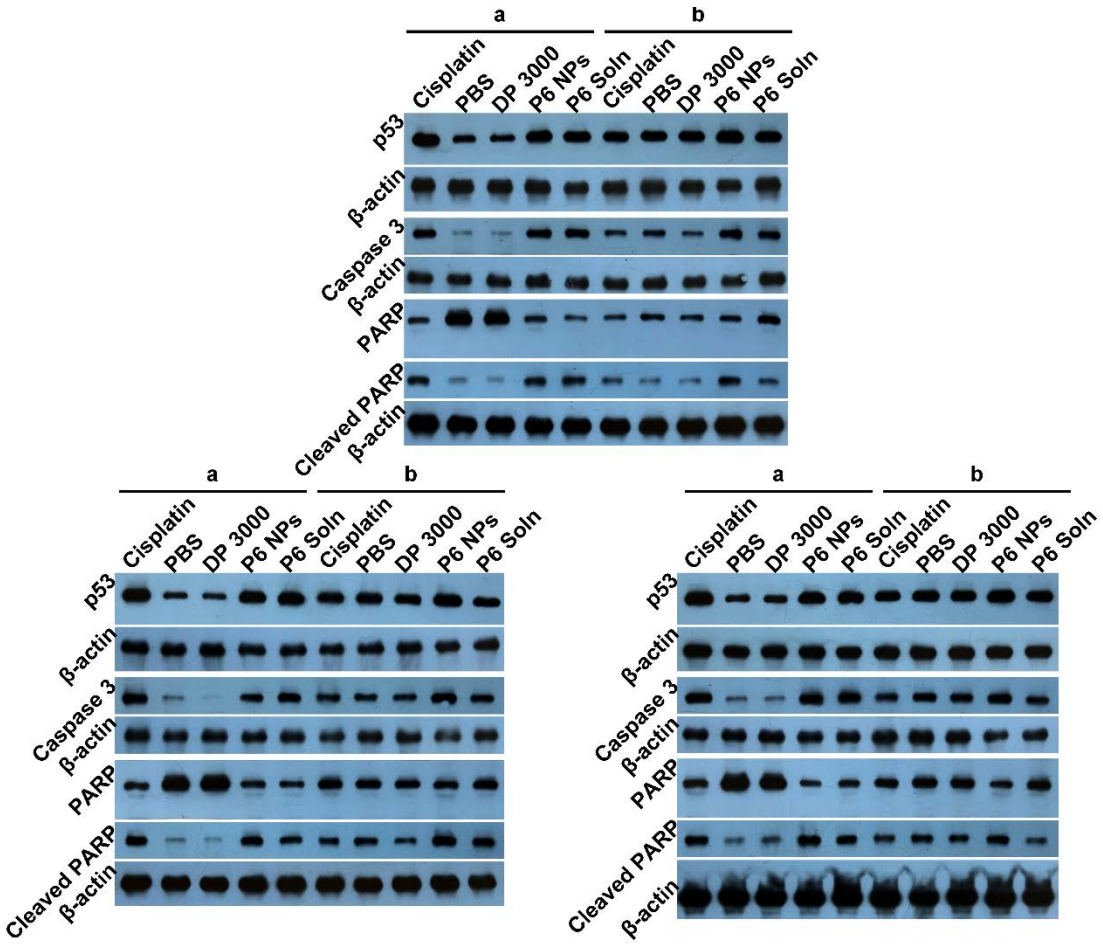

Figure S30. Western blot of p53, Caspase 3, PARP, and cleaved PARP in tumors harvested from (**a**) A2780 and (**b**) A2780cis tumor-bearing athymic nude mice after chemotherapy (n = 3).

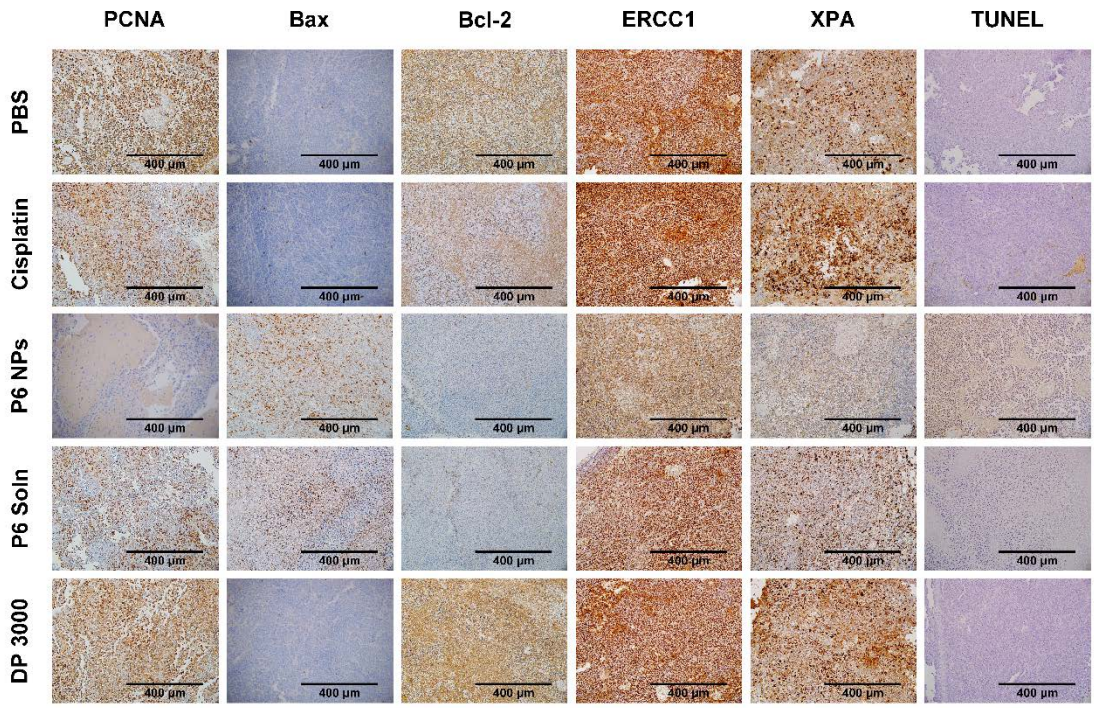

Figure S31. IHC and TUNEL images for A2780 xenograft tumors following treatment with PBS, cisplatin, P6 NPs, P6 Soln, or DP 3000. P6 NPs achieved cancer cell death after Pt-DNA adduct formation.

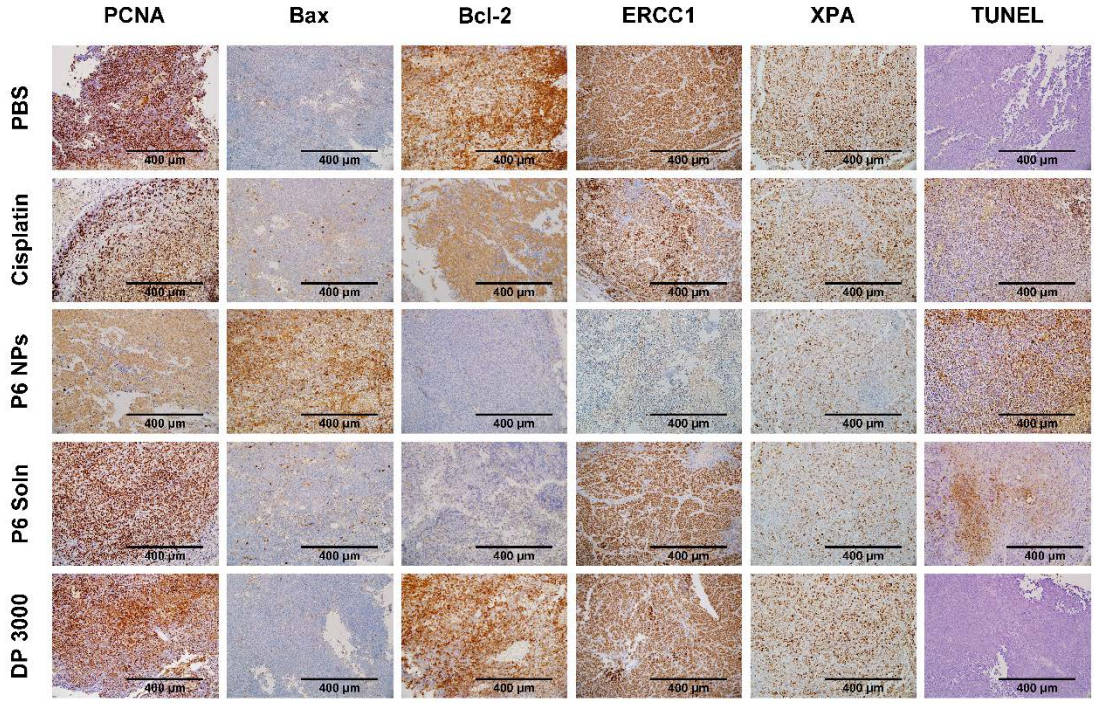

Figure S32. IHC and TUNEL images for A2780cis xenograft tumors following treatment with PBS, cisplatin, P**6** NPs, P**6** Soln, or DP 3000. P6 NPs achieved cisplatin-resistant cancer cell death after Pt-DNA adduct formation.

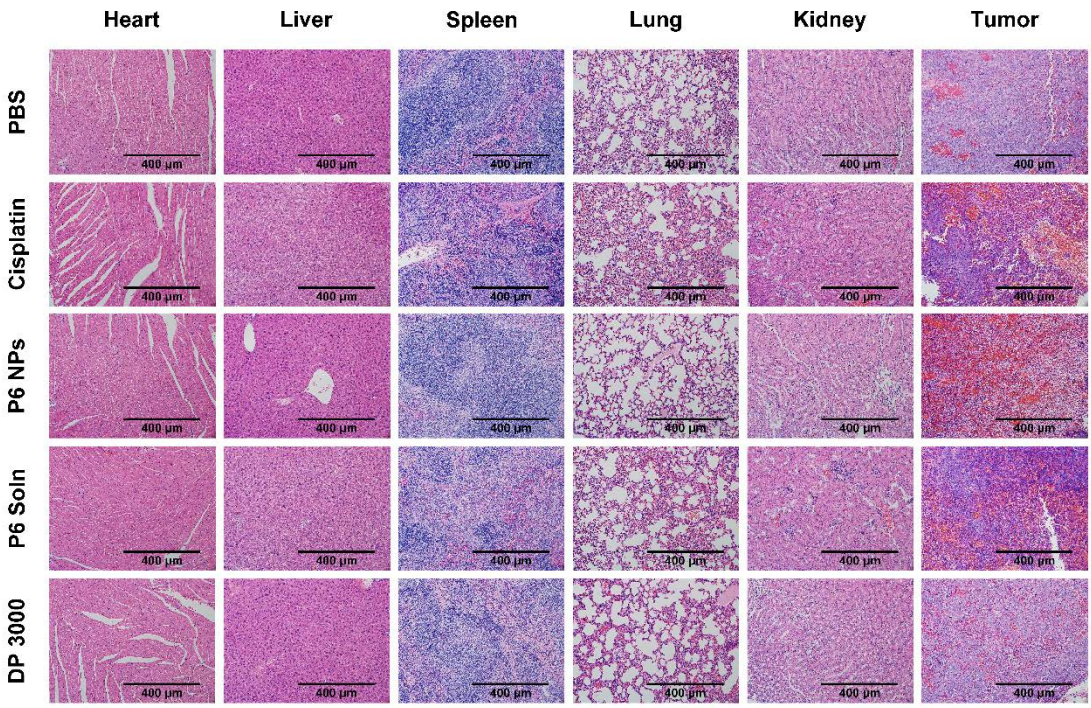

Figure S33. *Ex vivo* histological sections with H&E staining. Organs and tumors were harvested from A2780 tumor-bearing athymic nude mice after chemotherapy.

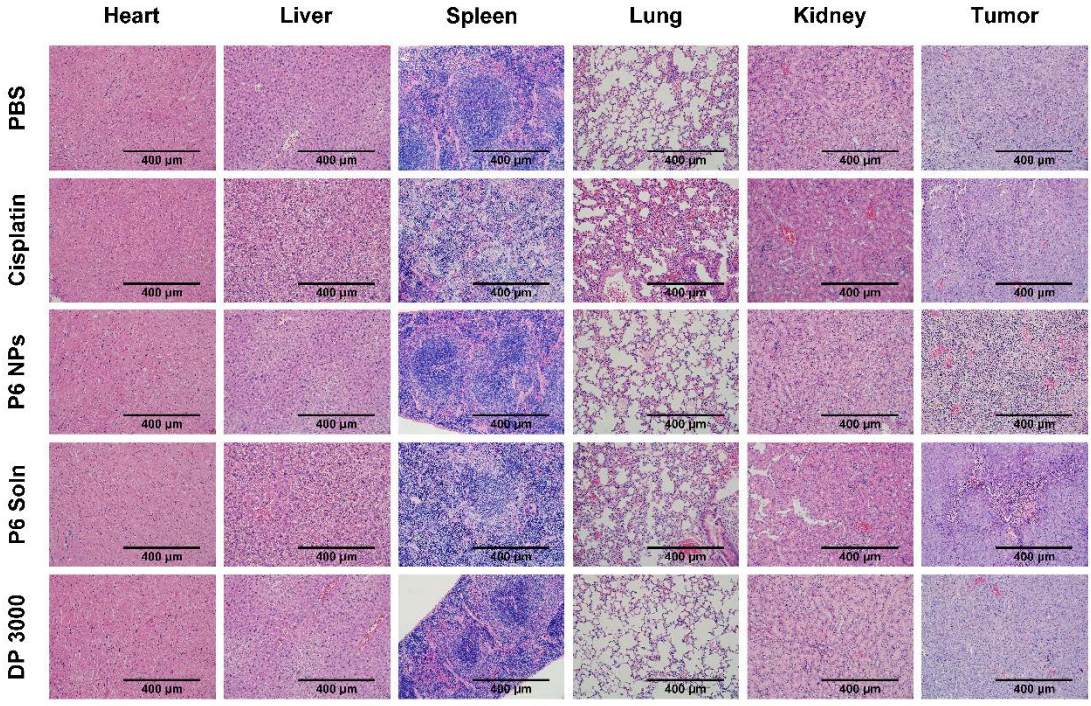

Figure S34. *Ex vivo* histological sections with H&E staining. Organs and tumors were harvested from A2780cis tumor-bearing athymic nude mice after chemotherapy.

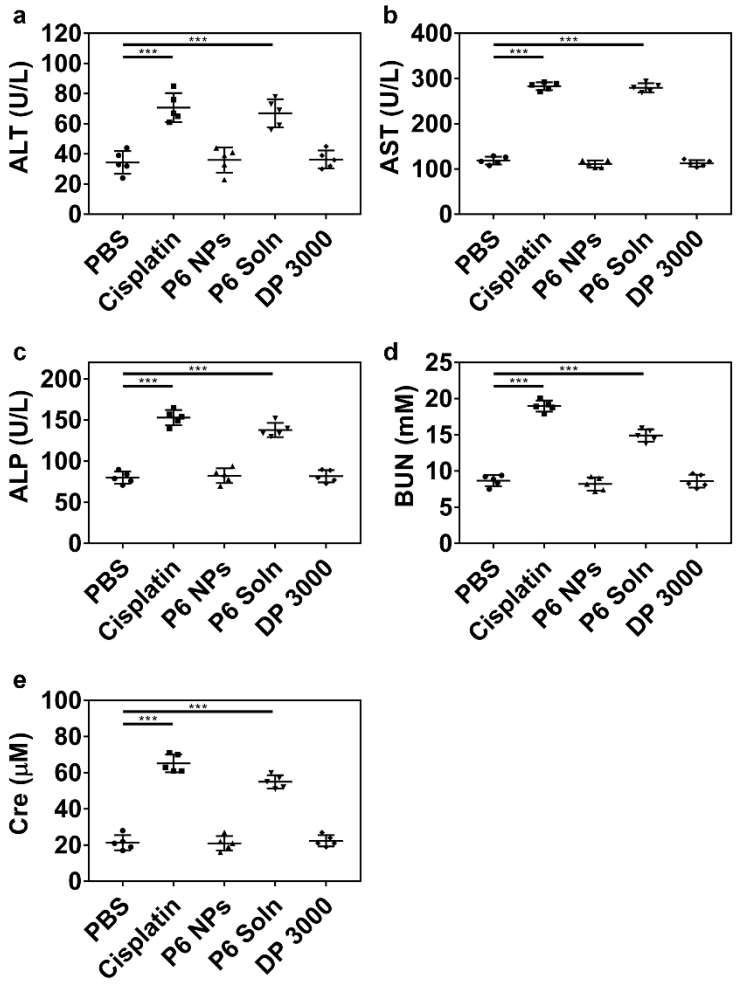

Figure S35. (**a**) ALT, (**b**) AST, (**c**) ALP, (**d**) BUN, and (**e**) Cre levels in serum collected from A2780 tumor-bearing athymic nude mice after chemotherapy (n = 5).

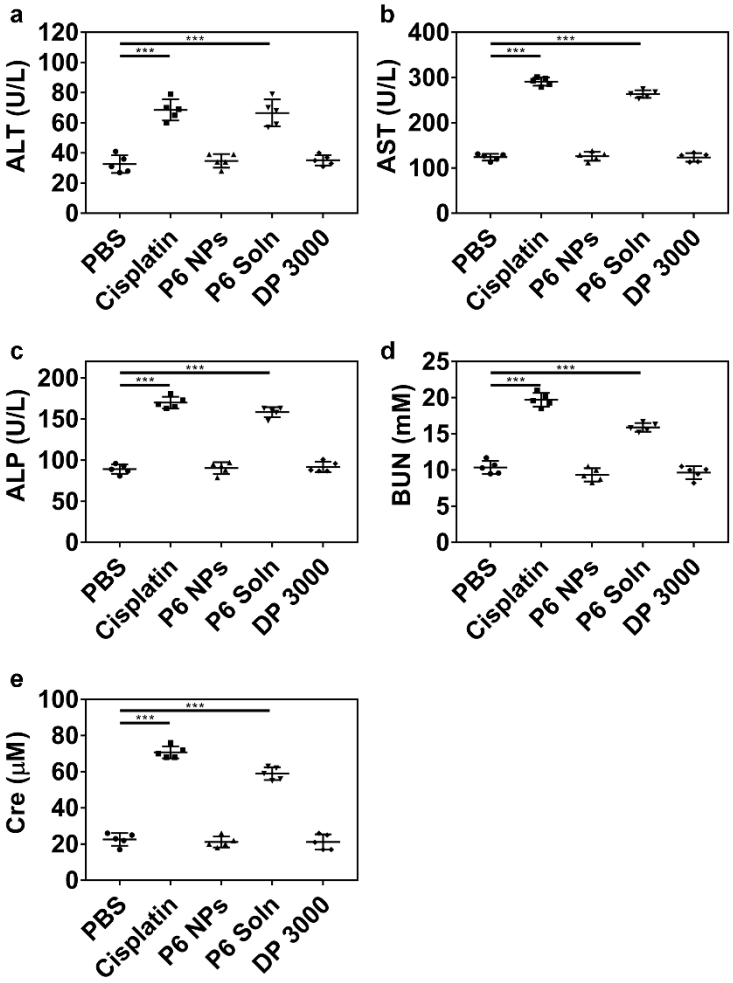

Figure S36. (**a**) ALT, (**b**) AST, (**c**) ALP, (**d**) BUN, and (**e**) Cre levels in serum collected from A2780cis tumor-bearing athymic nude mice after chemotherapy (n = 5).

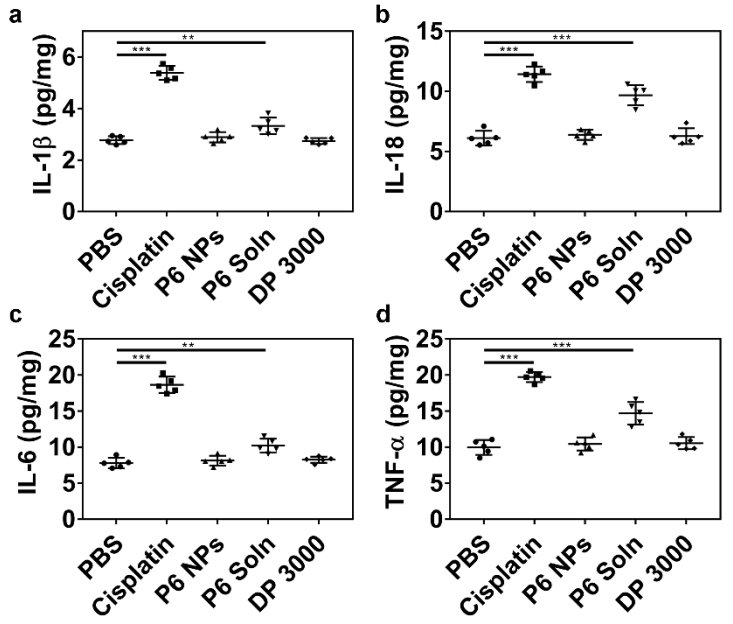

Figure S37. Renal levels of (**a**) IL-1β, (**b**) IL-18, (**c**) IL-6, and (**d**) TNF-α on day 1 from BALB/c mice post a single *i.v.* injection of PBS, cisplatin, P**6** NPs, P**6** Soln, or DP 3000 (n = 5).

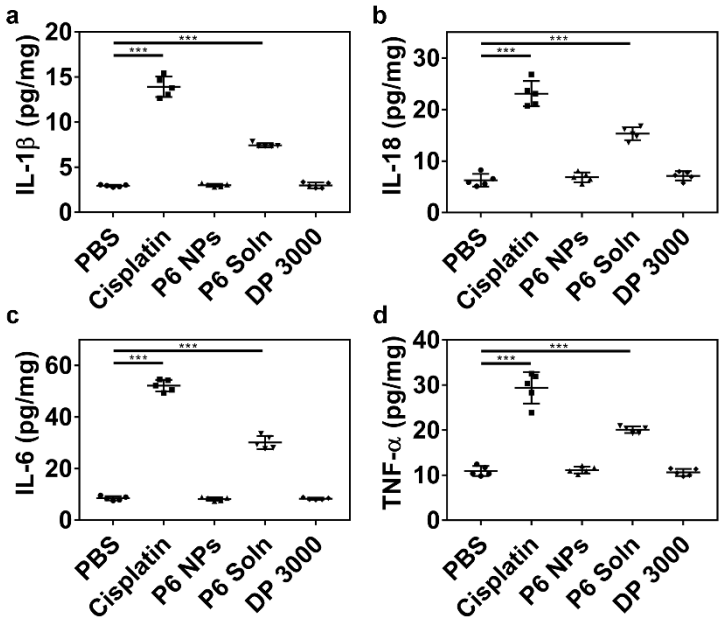

Figure S38. Renal levels of (**a**) IL-1β, (**b**) IL-18, (**c**) IL-6, and (**d**) TNF-α on day 3 from BALB/c mice post a single *i.v.* injection of PBS, cisplatin, P**6** NPs, P**6** Soln, or DP 3000 (n = 5).

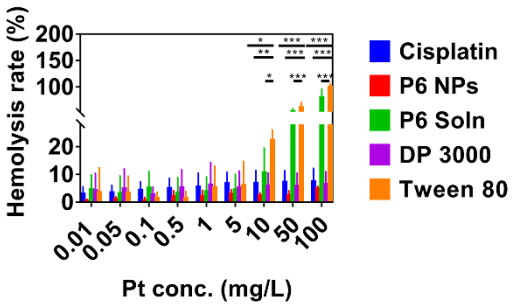

Figure S39. Hemolysis rate of cisplatin, P**6** NPs, P**6** Soln, DP 3000, and Tween 80.

Table S1. Pt(IV) **1-8** and their corresponding NPs.

Pt(IV) prodrugs	Acid anhydride	n*	Abbreviation of NPs
Pt(IV) **1**	Acetic anhydride	0	P**1** NPs
Pt(IV) **2**	Butanoic anhydride	2	P**2** NPs
Pt(IV) **3**	Hexanoic anhydride	4	P**3** NPs
Pt(IV) **4**	Octanoic anhydride	6	P**4** NPs
Pt(IV) **5**	Decanoic anhydride	8	P**5** NPs
Pt(IV) **6**	Dodecanoic anhydride	10	P**6** NPs
Pt(IV) **7**	Tetradecanoic anhydride	12	P**7** NPs
Pt(IV) **8**	Hexadecanoic anhydride	14	P**8** NPs

* The number of methylene spacers shown in Figure S1.

Table S2. Particle size, zeta potential, and Pt loading of NPs prepared from Pt(IV) **1-8**.

Obtained NPs	Particle size (nm)	Polydispersity index	Zeta potential (mV)	Pt loading (%)*
P**1** NPs	45.6±0.6	0.259±0.014	2.210±1.520	0.50±0.07
P**2** NPs	69.9±0.9	0.284±0.002	1.910±2.400	1.12±0.15
P**3** NPs	74.8±0.8	0.268±0.007	1.890±1.160	2.06±0.16
P**4** NPs	90.7±0.5	0.271±0.009	0.117±0.166	9.53±0.61
P**5** NPs	96.6±2.1	0.266±0.005	-0.407±0.232	10.53±0.97
P**6** NPs	99.3±0.7	0.228±0.006	-0.441±0.456	11.24±0.10
P**7** NPs	124.7±2.7	0.247±0.019	-1.550±0.745	14.29±0.48
P**8** NPs	158.7±1.3	0.269±0.005	-3.310±2.780	12.67±0.61

* Pt loading was calculated according to the equation: Pt loading (%) = Weight of charged Pt/Weight of NPs × 100.

Table S3. Pharmacokinetics of BALB/c mice post a single intravenous injection of cisplatin, P**6** NPs, or P**6** Soln.

Model type	Parameters	Unit	Cisplatin	P**6** NPs	P**6** Soln
Non-compartment model	$AUC_{0\rightarrow inf}$	(h·mg)/L	44.91±11.08	158.55±27.59	168.35±44.29
	$AUMC_{0\rightarrow inf}$	(h·h·mg)/L	345.54±120.67	4381.03±717.26	2676.82±719.09
	CL	L/(h·kg)	0.11±0.02	0.03±0.01	0.03±0.01
	V_{ss}	L/kg	0.79±0.11	0.81±0.15	0.45±010
	$MRT_{0\rightarrow inf}$	h	7.57±0.73	27.66±0.50	15.89±0.08
Two-compartment model	A	mg/L	70.01±9.98	52.65±5.44	55.79±9.84
	α	h^{-1}	7.08±0.64	2.43±0.42	3.45±0.55
	B	mg/L	14.31±4.77	10.16±1.51	14.93±2.90
	β	h^{-1}	0.84±0.05	0.13±0.02	0.15±0.01
	$t_{1/2\alpha}$	h	0.10±0.01	0.29±0.06	0.20±0.04
	$t_{1/2\beta}$	h	0.82±0.05	5.39±0.67	4.56±0.38
	k_{10}	h^{-1}	3.20±0.48	0.63±0.06	0.62±0.07

	k_{12}	h^{-1}	2.83±0.27	1.42±0.28	2.14±0.38
	k_{21}	h^{-1}	1.88±0.24	0.50±0.11	0.85±0.12

Table S4. Tumor inhibition rate (TIR) of A2780 and A2780cis tumor-bearing athymic nude mice after chemotherapy.

TIR (%)	Cisplatin	P**6** NPs	P**6** Soln	DP 3000
A2780 xenograft model	84.71±0.92	85.99±2.78	71.28±14.73	17.34±16.09
A2780cis xenograft model	12.65±71.44	88.69±3.33	72.82±13.20	9.42±40.17